

## **CHAPTER - 4**

***Attempts to synthesize  
propeller-shaped triple  
helixes***

## Table of Contents

<b>4.1</b>	<b>Introduction to multiple [n]helicenes</b>	<b>189</b>
<b>4.2</b>	<b>Chemistry of Triple helicenes: Literature insight</b>	<b>189-193</b>
<b>4.3</b>	<b>Results and Discussion</b>	<b>193-203</b>
<b>4.3.1</b>	Attempted synthesis of triple aza[6]helicene	193-196
<b>4.3.2</b>	Attempted synthesis of triple 1,3-dimethyl[4]helicene	197-201
<b>4.3.3</b>	Attempt to synthesize propeller-shaped triple helical oxazine	201-203
<b>4.4</b>	<b>Conclusion</b>	<b>204</b>
<b>4.5</b>	<b>Experimental data</b>	<b>205-213</b>
<b>4.6</b>	<b>Spectral data</b>	<b>214-220</b>
<b>4.7</b>	<b>Computational data</b>	<b>221-223</b>
<b>4.8</b>	<b>References</b>	<b>224-226</b>

## 4.1 Introduction to multiple [n]helicenes

Multiple [n]helicenes are composed of more than one mono[n]helicene subunit. When compared to the traditional mono[n]helicenes, these multiple [n]helicenes possess many unique properties along with their characteristic cores.<sup>1</sup> In case of multiple helicenes, extremely twisted polyaromatic rings can be built, which reveals the limits of aromaticity as well as the  $\pi$  bonds. Also, multiple helicenes becomes a subject of special interest as they possess structural beauty, multiple chiral units and unique dynamic behavior which leads to synthetic challenges.<sup>2</sup> Moreover their photophysical properties can be tuned by making changes either in their core or the number of [n]helicenes. The multiple [n]helicenes consists of a larger  $\pi$ -conjugated system compared to the mono[n]helicenes, leading to some unique molecular packing arrangements and self-assembly behavior. Lastly, multiple helicenes exhibit various stable conformers, and these conformational differences often lead to significant variations in their topological structure, physicochemical properties, and molecular packing, which enables them to be used as models in investigating their stereochemistry. Owing to these properties they show potential applications as: spin filters,<sup>3</sup> circularly polarized light (CPL) emitters in OLEDs,<sup>4</sup> and photoswitches.<sup>5</sup>

## 4.2 Chemistry of Triple helicenes: Literature insight

It is a class of multiple helicenes, where three helicene units co-exists in the same molecule. The symmetric triple helicenes has become a topic of interest in the field of research as they possess unique characteristic properties along with the structural beauty and have been synthesized by employing different synthetic procedures in the literature.

These symmetric triple helicenes possess four isomers: two pairs of enantiomers [(P,P,P), (M,M,M) and (P,P,M) and (P,M,M)]. The representative member of this type of multiple helicene is the triple [5]helicene **1**, in (P,P,P) conformation. (**Figure 4.1**)

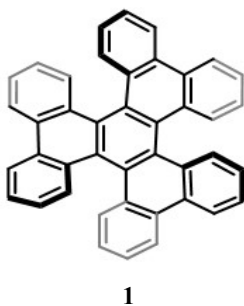


**Figure 4.1:** Figure showing reported symmetric triple [5]helicene

McOmie and co-workers were the first to report the synthesis of **1** in 1982 by the pyrolysis of cyclobuta[1]phenanthrene-1,2-dione under vacuum, where the detailed structural characteristics were not studied.<sup>6</sup> Later in 1999, synthesis of **1** was reported by two other groups independently. Pascal and co-workers employed flash vacuum pyrolysis of phenanthrene-9,10-dicarboxylic anhydride to obtain the triple [5]helicene **1**. A  $D_3$ -symmetric structure **1a** was assigned on the basis of X-ray crystallography.<sup>7</sup> A Pd-catalyzed cyclotrimerization of 9,10-didehydrophenanthrene was used to synthesize **1** by Pérez, Guitián and co-workers.<sup>8</sup> Later, the conformational study of **1** was carried out by the same group which revealed that a metastable  $C_2$  conformer **1b** was obtained. Also, isomerization barriers of 11.7 kcal·mol<sup>-1</sup> (**1b** → **1b\***) and 26.2 kcal·mol<sup>-1</sup> (**1b** → **1a**) were determined experimentally (Figure 4.2).<sup>9</sup>

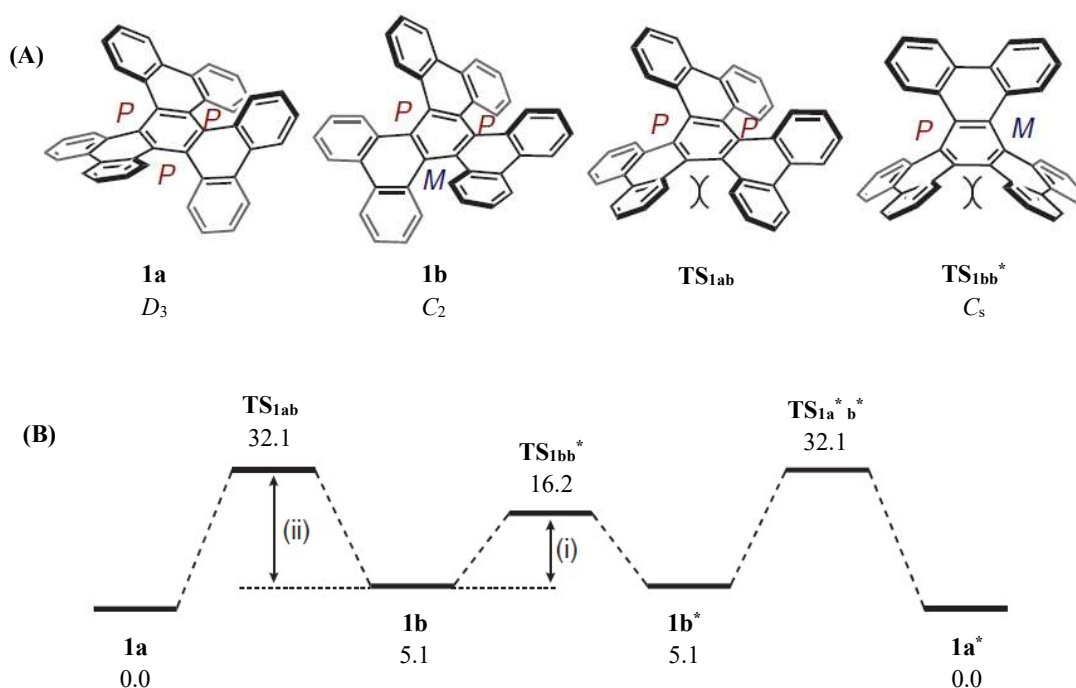
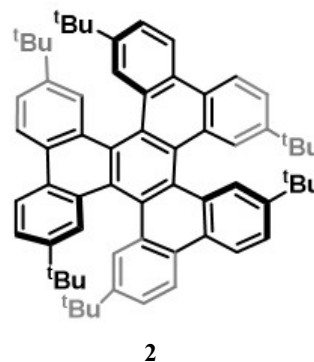


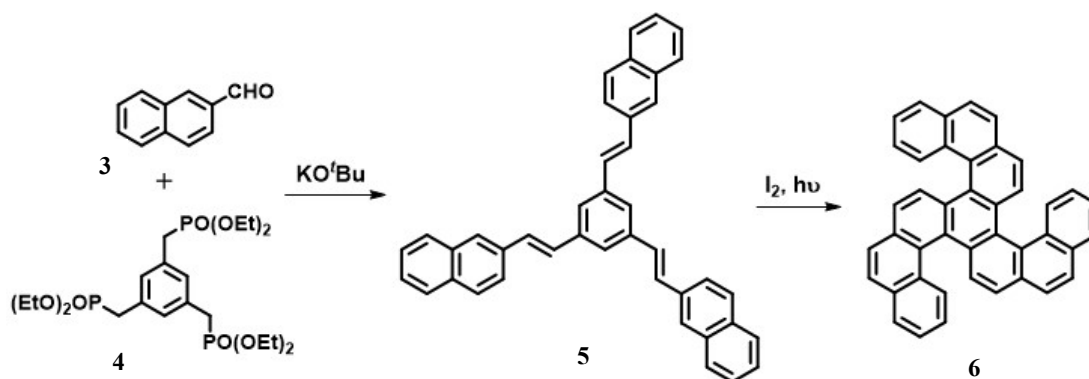
**Figure 4.2:** (A) Optimized conformers and transition structures of **1**. (B) Racemization pathway of **1** with relative Gibbs free energy values (kcal·mol<sup>-1</sup>).

The racemization pathway of the triple helicene **1** reveals that  $D_3$  symmetric structures **1a** and **1a\*** are the most stable conformations of **1** (Figure 4.2 (B)). The enantiomerization from **1a** to **1a\*** proceeded via **1a** → **1b** → **1b\*** → **1a\***, where **1a** → **TS<sub>1ab</sub>** ( $\Delta G = 32.1$  kcal·mol<sup>-1</sup>) was observed as the rate-determining step. In this pathway, the original chirality ( $P,P,P$ ) of **1a** was lost upon transformation into the  $C_s$  symmetric transition state **TS<sub>1bb\*</sub>**. The structural characterization of **1b** was carried out by Wenger and coworkers by using X-ray crystallography.<sup>10</sup>

In 2011, Durola and co-workers reported the synthesis of **2**, which is a hexa-*tert*-butylated derivative of **1**.<sup>11</sup> They used a strategy where 1,3,5-tribromobenzene was modified directly *via* three-fold Suzuki-Miyaura coupling reactions with 4,4'-ditert-butylbiphenyl to construct the precursor of **2**, followed by Scholl reaction. Helicene **2** exhibited a  $D_3$  symmetry and showed a propeller-shaped geometry.



In 2017, Watanabe and co-workers reported the synthesis of another type of triple [5]helicene **6** by an oxidative photocyclization reaction (**Scheme 4.1**).<sup>12</sup>



**Scheme 4.1:** Synthesis of triple [5]helicene **6** by oxidative photocyclization

Compound **6** was expected to exist as two diastereomers: *P,P,P* (or its enantiomer, *M,M,M*) and *P,P,M* (or its enantiomer, *P,M,M*), where *P* or *M* indicates the helicity of one [5]helicene unit. The HPLC analysis over a chiral column indicated that the enantiomers *P,P,P* and *M,M,M* were present in 1:1 ratio, which were separated and found to be stable at room temperature.

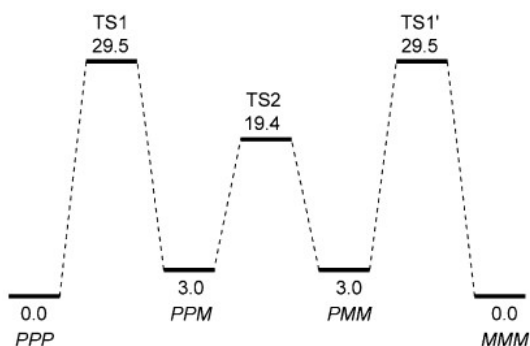
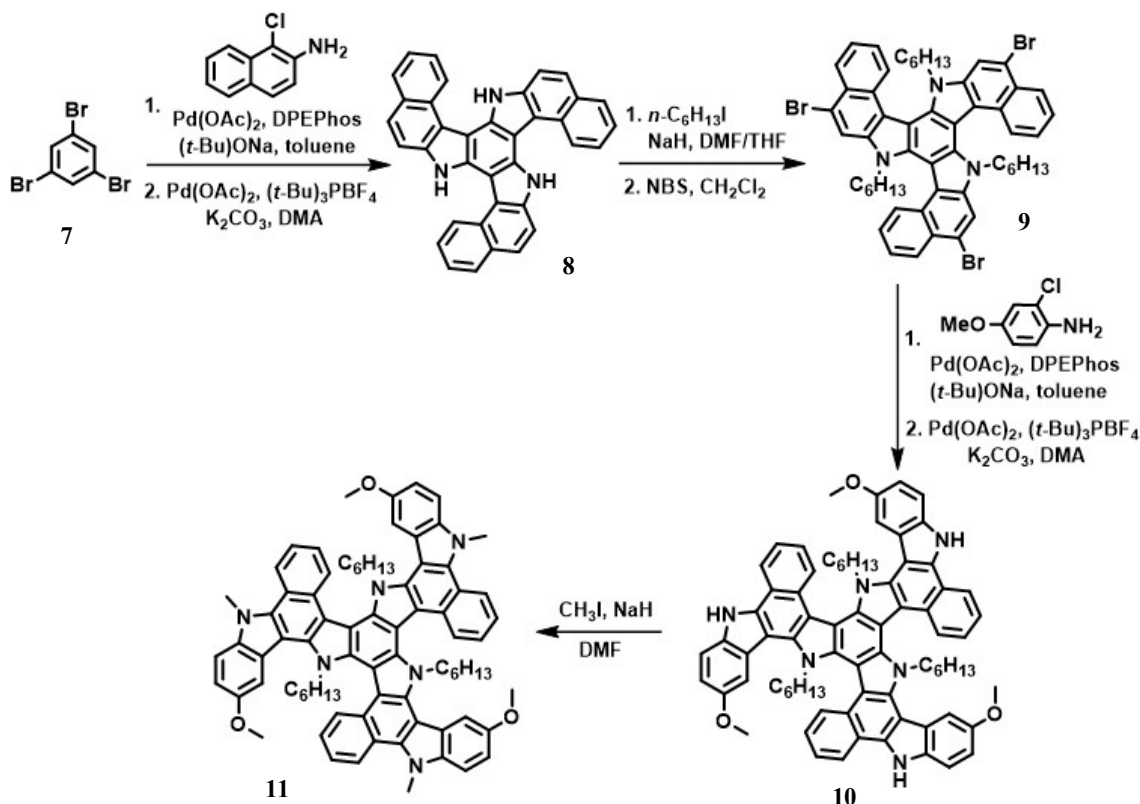


**Figure 4.3:** Energy profile diagram for the isomerization of triple [5]helicene **6**, as estimated by DFT calculations<sup>12</sup>

The isomerization and racemization processes were studied by DFT calculations which revealed that the isomer *P,P,P* (or *M,M,M*) is thermodynamically more stable than (*P,P,M*)-**6** by 3 kcal·mol<sup>-1</sup>. The calculated racemization barrier of **6** was found to be 29.5 kcal·mol<sup>-1</sup> (**Figure 4.3**). Also, (*P,P,M*)-**6** isomerized to the more stable (*P,P,P*)-**6** conformation at room temperature with a half-life of 2.3 days which was determined by <sup>1</sup>H NMR.

Recently, in 2022, Wang and co-workers reported a triple helicene based molecular semiconductor **11** where the helicene scaffold was synthesized from 1,3,5-tribromobenzene by employing multiple Buchwald-Hartwig amination as the key steps (**Scheme 4.2**).<sup>13</sup>



**Scheme 4.2:** Synthesis of triple [5]helicene **11**

Two furan-based triple helicenes were reported by two different group of scientist independently. In 2021, Yang and co-workers reported the synthesis of triple oxa[7]helicene **12** by a [2+2+2] cyclotrimerization of dibenzofuryl acetylene followed by intramolecular dehydrogenative annulation. They compared **12** with the previously reported double oxa[7]helicene. It was observed that the triple oxa[7]helicene **12** showed enhanced luminescence dissymmetry factors were observed in both theoretical and experimental studies.

These investigations suggested that helicene subunit multiplication is a key to improving the dissymmetry factors in the heterohelicenes.<sup>14</sup>

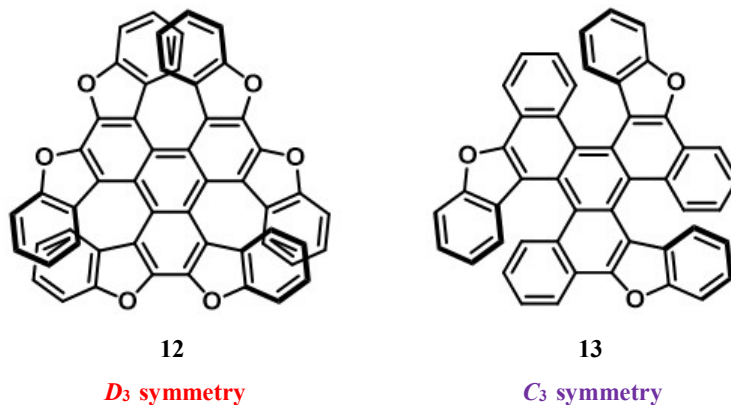


**Figure 4.4:** Figure showing reported furan-based triple helicenes

Later in 2022, a  $C_3$ -symmetric triple oxa[6]helicene **13** was synthesized by Hu and co-workers by a two-step procedure involving a triple Suzuki-Miyaura coupling of 1,3,5-tri(2-bromophenyl)benzene with benzofuran-2-boronic acid, followed by a Scholl reaction. The authors revealed that in contrast to the  $D_3$ -symmetric triple oxa[7]helicene **12**, more pronounced luminescence dissymmetry factors were observed in case of  $C_3$ -symmetric triple oxa[6]helicene **13**. This suggested that the molecular symmetry plays a significant role on the chiroptical response of triple helicenes.<sup>15</sup>

Thus, these interesting properties and potential applications of triple helicenes inspired us to undertake the synthesis of few triple helicenes. There are very few reports in the literature where oxidative photocyclization is used for the synthesis of such molecules. In this chapter we present our efforts towards the synthesis of triple helicenes.

## 4.3 Results and Discussion

### 4.3.1 Attempted synthesis of triple aza[6]helicene

The retrosynthetic scheme for triple aza[6]helicene was designed as shown in **Figure 4.5**. The synthesis of the target molecule could be achieved by oxidative photocyclization of the corresponding tris-olefin derivative obtained by the Heck reaction between the starting materials 1,3,5-tribromobenzene and 3-vinyl *N*-butyl carbazole which can be synthesized easily in large scale.

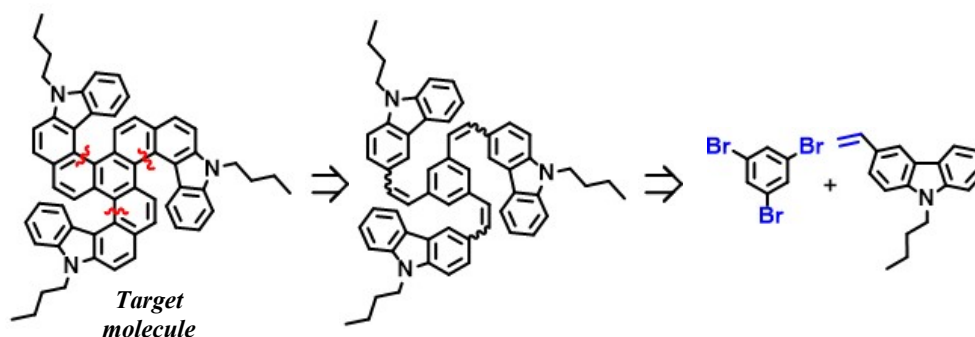
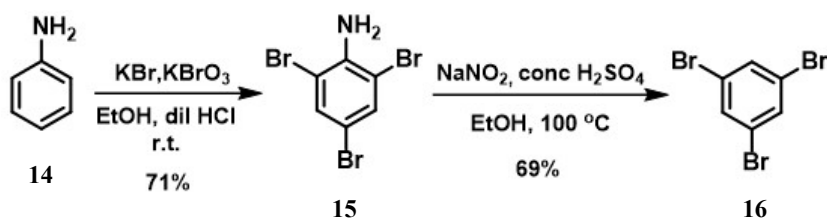


**Figure 4.5:** Retrosynthetic analysis of triple aza[6]helicene

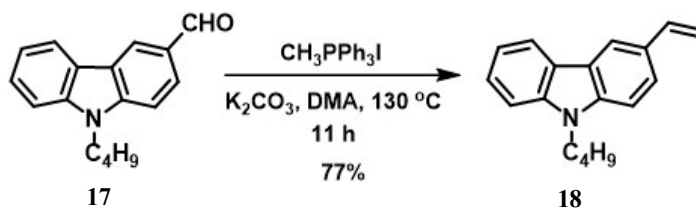
#### 4.3.1.1 Synthesis of the tris-olefin precursor 19

In order to synthesize the tris-olefin by Mizoroki-Heck reaction, two counterparts need to be synthesized. 1,3,5-tribromobenzene **16** was synthesized in two steps (**Scheme 4.3**), where the first step involved the bromination of aniline to obtain 2,4,6-tribromobenzene **15**. This was followed by the deamination step where the amine **15** was converted into the diazonium salt in ethanol solution, which on heating brings about the reductive removal of the diazo group as ethanol is oxidised to acetaldehyde.



**Scheme 4.3:** Synthesis of 1,3,5-tribromobenzene

The other starting material **18**, was synthesized by the well-known Wittig olefination reaction between the 3-formyl *N*-butyl carbazole **17** which can be synthesized in gram scale with the methyl triphenylphosphonium iodide prepared from methyl iodide and triphenyl phosphine (**Scheme 4.4**).

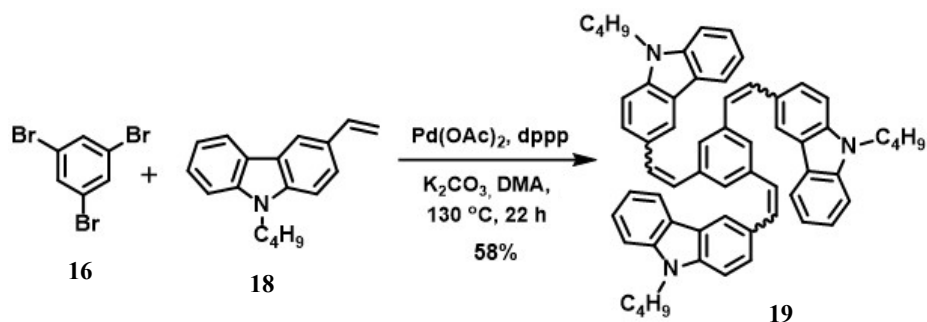


**Scheme 4.4:** Synthesis of 3-vinyl *N*-butyl carbazole

This 1,3,5-tribromobenzene **16** was then subjected to triple Heck reaction with 3-vinyl *N*-butyl carbazole **18**, to obtain the corresponding tris-olefin **19** as mixture of *E/Z* forms (**Scheme**



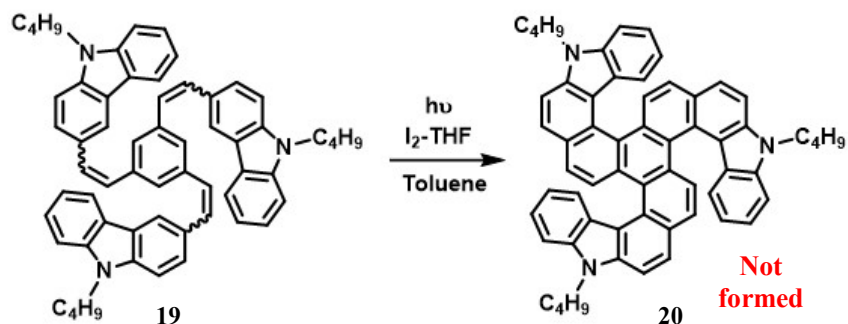
4.5). The formation of this tris-olefin was confirmed by the  $^1\text{H}$  NMR, which showed only one set of signals in the aliphatic region indicating that the Heck reaction has occurred on three sides. Also, the presence of doublet at 7.12 ppm (16.4 Hz), which confirms the presence of *E*-isomer, which was formed in major amount.



**Scheme 4.5:** Synthesis of tris-olefin **19**

#### 4.3.1.2 Attempted photocyclization of tris-olefin **19**

The tris-olefin **19** was subjected to oxidative photocyclization under 125 W HPMVL, in toluene using iodine and tetrahydrofuran (**Scheme 4.6**). The reaction did not result into the formation of the expected product **20**. It is observed that these photocyclization reactions depend on the concentration of the starting material and capacity of HPMVL. Then, various experiments were performed by either lowering the concentration or changing the capacity of the HPMVL or continuing the reaction for extended time (**Table 4.1**).



**Scheme 4.6:** Attempted photocyclization of **19**

No.	Capacity of HPMVL (W)	Concentration of <b>19</b> (M)	Time (h)
1	125	$1.5 \times 10^{-4}$	11
2	125	$1.7 \times 10^{-6}$	11
3	125	$1.7 \times 10^{-6}$	24
4	250	$1.5 \times 10^{-4}$	8
5	250	$1.7 \times 10^{-6}$	15

**Table 4.1.:** Attempted variations in the reaction conditions

But none of these conditions led to the formation of the desired product, only a sticky mass was obtained in all the cases. The  $^1\text{H}$  NMR of this material showed the absence of doublet at 7.12 ppm corresponding to the olefinic proton in the olefin **19**, indicating complete consumption of the starting material (**Figure 4.6 (B)**). However, we were unsuccessful in predicting the exact structure of the isolated material.

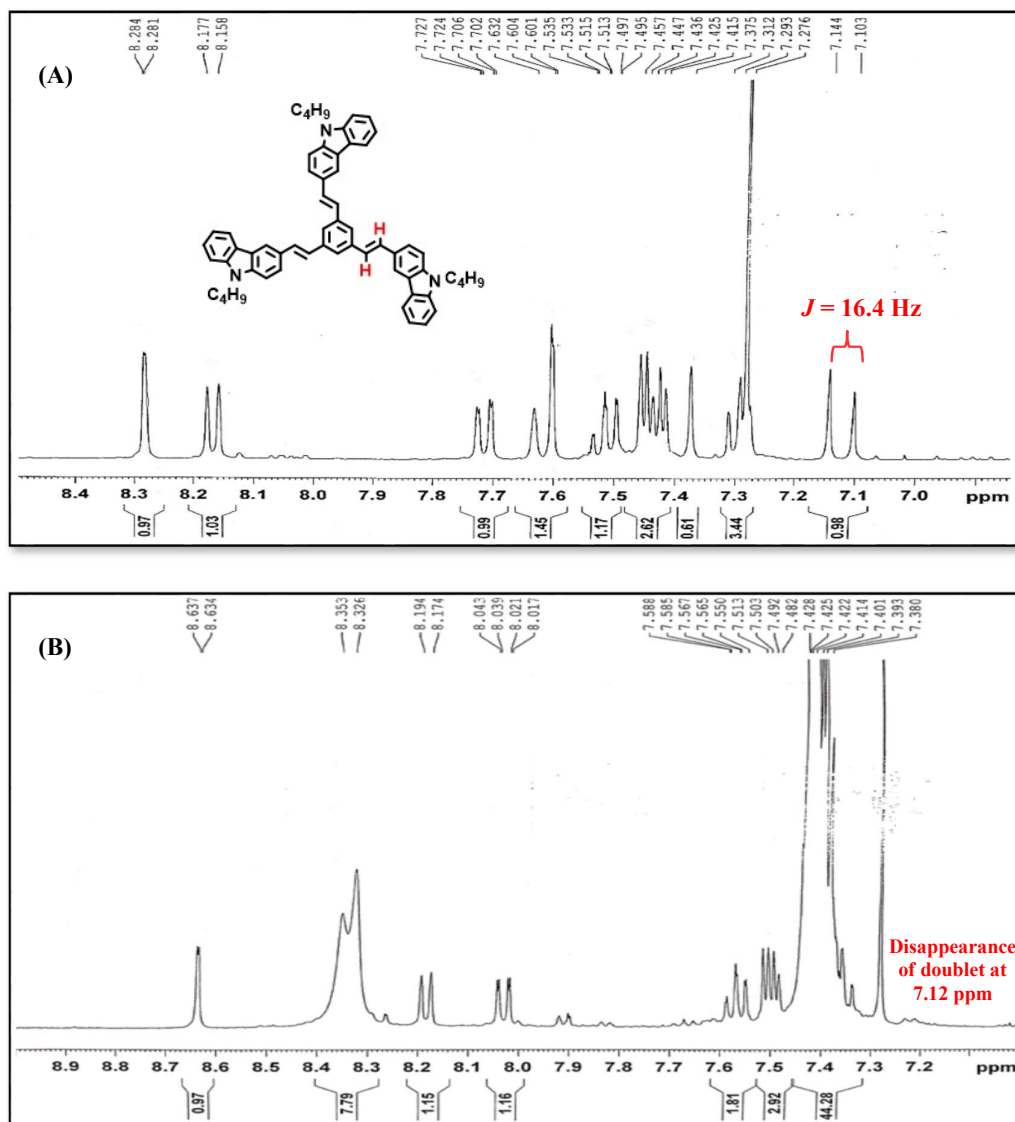


**Figure 4.6:** Comparison of (A)  $^1\text{H}$  NMR Spectrum of **19** (Enlarged aromatic region) ( $\text{CDCl}_3$ , 400 MHz) (B)  $^1\text{H}$  NMR Spectrum of material isolated from photocyclization reaction in  $\text{CDCl}_3$  (Enlarged aromatic region)

We believe that these difficulties in the photocyclization step might have occurred due to the presence of three bulky carbazole units. Thus we shift our focus to some smaller systems.

### 4.3.2 Attempted synthesis of triple 1,3-dimethyl[4]helicene

Triple 1,3-dimethyl[4]helicene **27**, comparatively a smaller moiety with lesser steric strain was chosen as the target molecule. But the problem with the smaller helicenes is their low configurational stability. Smaller helicenes like [4]helicene without any substitution in the fjord region, does not intrinsically adopt the helical topology as they lack the overlap of the terminal rings. Thus, they have almost flat structures. However, they can be studied for their application in material science due to good emissive properties and enhanced conjugation. Moreover, it is known that by introducing some bulky substituents capable of increasing the steric hindrance can improve the configurational stability of smaller order of helicenes. Literature shows few reports wherein introduction of methyl substituent in the fjord region sufficiently increases the barrier of racemization by a considerable extent (**Figure 4.7**).<sup>16</sup>

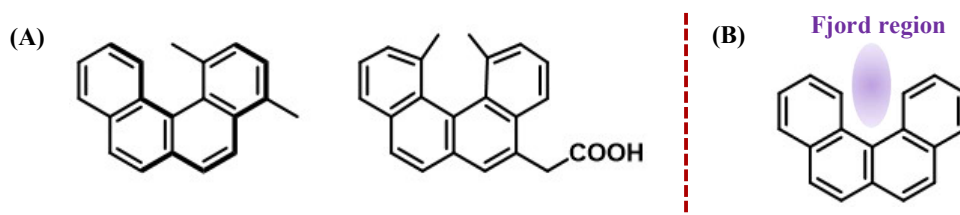


**Figure 4.7:** (A) Some reported configurationally stable [4]helicenes (B) Figure explaining the fjord region in helicenes

Thus, the target molecule was designed such that there is lesser steric strain during the photocyclization step, also the presence of methyl group in the fjord region increases the configuration stability, providing a twist in the [4]helicene unit. The triple helicene **27** can be synthesized by oxidative photocyclization of the corresponding tris-olefin which could be obtained as a product of Heck reaction between 1,3,5-tribromobenzene and 3,5-dimethylstyrene (**Figure 4.8**).

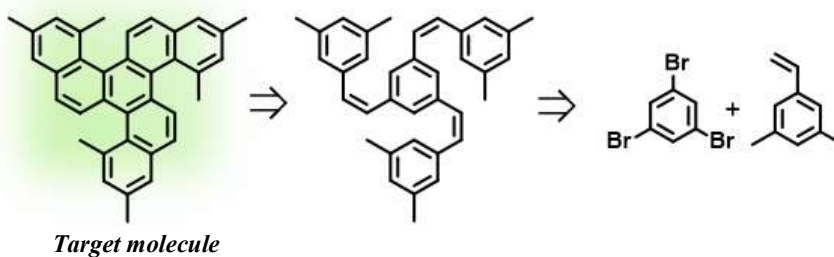
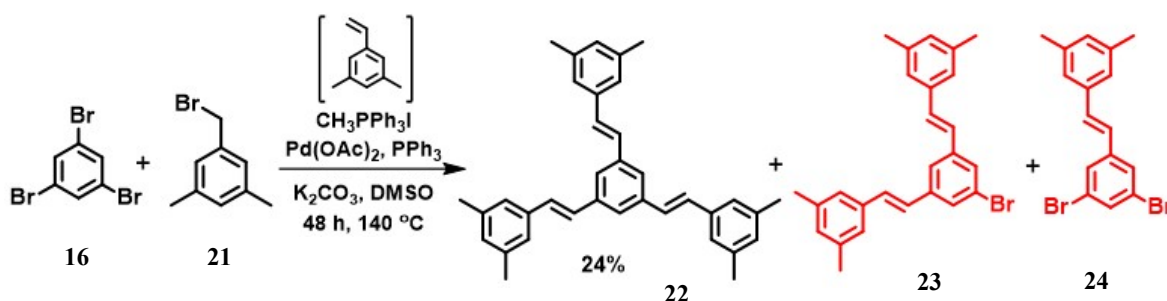


**Figure 4.8:** Retrosynthetic analysis of triple 1,3-dimethyl[4]helicene

#### 4.3.2.1 Synthesis of tris-olefin **22**

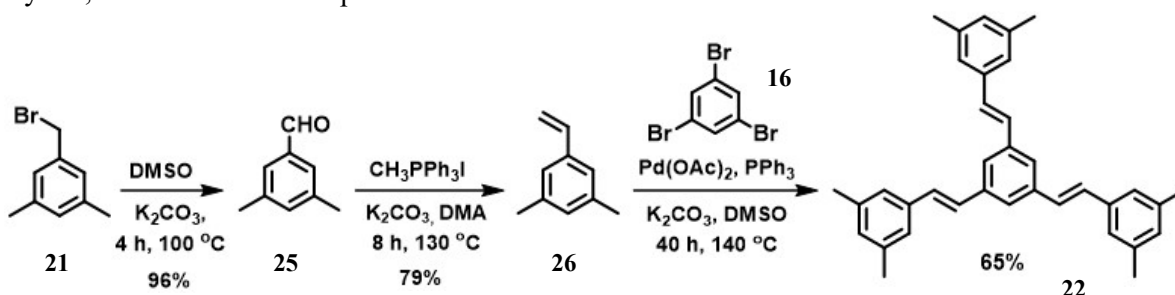
In order to reach the target molecule, we first carried out the synthesis of the tris-olefin

**22.** Our first strategy was one-pot oxidation-Wittig-Heck reaction which was earlier established in our lab.<sup>17</sup> The required 3,5-dimethyl benzyl bromide **21** was prepared by the side chain bromination of mesitylene. This was then subjected to the one-pot reaction sequence with 1,3,5-tribromobenzene **16**, in addition to methyl triphenylphosphonium iodide, palladium acetate, triphenylphosphine, and potassium carbonate as base in dimethyl sulfoxide, where the 3,5-dimethylstyrene **26** is generated insitu (**Scheme 4.7**). After the completion of the reaction, multiple spots were observed on TLC, out of which three major spots were isolated and purified by column chromatography. It was observed that along with our desired tris-olefin **22**, mono-olefin **24** and bis-olefin **23** were also formed. Their formation was confirmed by <sup>1</sup>H NMR. They were distinguished by the number of protons of the methyl group and the number of olefinic protons. A unique observation was made in the <sup>1</sup>H NMR of **22**, where the two olefinic protons appeared as a 's' and did not show any splitting. By this strategy, we could not achieve exact control over the exclusive formation of **22**.



**Scheme 4.7:** Synthesis of olefin **22** by one-pot oxidation-Wittig-Heck

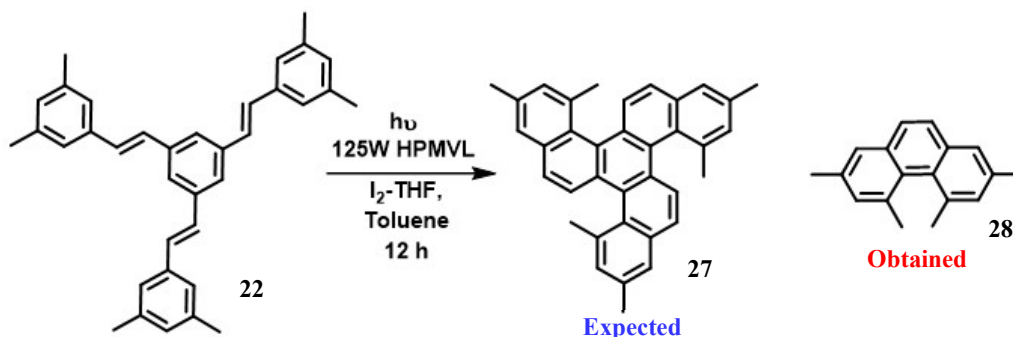
Then, we targeted the stepwise approach where the 3,5-dimethylstyrene **26** was synthesized in two steps, involving Kornblum oxidation of 3,5-dimethyl benzyl bromide **21** to obtain aldehyde **25**, followed by its Wittig olefination with the methyl triphenylphosphonium iodide. Styrene **26** was then isolated, purified and then subjected to Heck reaction with 1,3,5-tribromobenzene **16** (**Scheme 4.8**). In this case, the desired tris-olefin was obtained in good yield, while the other two products were formed in minor amount.



**Scheme 4.8:** Synthesis of olefin **22** by stepwise approach

### 4.3.2.2 Photocyclization of tris-olefin **22**

The tris-olefin **22** was subjected to oxidative photocyclization using 125 W HPMVL in presence of iodine and tetrahydrofuran in toluene and the reaction was continued till complete conversion of starting material **22** (Scheme 4.9). The crude reaction mass was subjected to column chromatography over silica gel, where only one pure compound was isolated. The purified compound was tested for its  $^1\text{H}$  NMR, which showed very few signals indicating the formation of a symmetrical compound. Additionally, the presence of two singlets in the aliphatic region made an illusion of the formation of our expected triple helicene **27**. But the mass analysis did not show any molecular ion peak corresponding to molecular weight of **27**.



**Scheme 4.9:** Photocyclization of **22**

In order to obtain the exact structure, we carried out its crystallization. A good quality crystal was obtained in dichloromethane solvent which was subjected to single crystal X-ray analysis. This X-ray diffraction study revealed the formation of 2,4,5,7-tetramethylphenanthrene **28** instead of our desired product **27**. The  $^1\text{H}$  NMR was also in favor of formation of **28** as it showed only three type of protons in the aromatic region and two type of methyl groups (Figure 4.9).

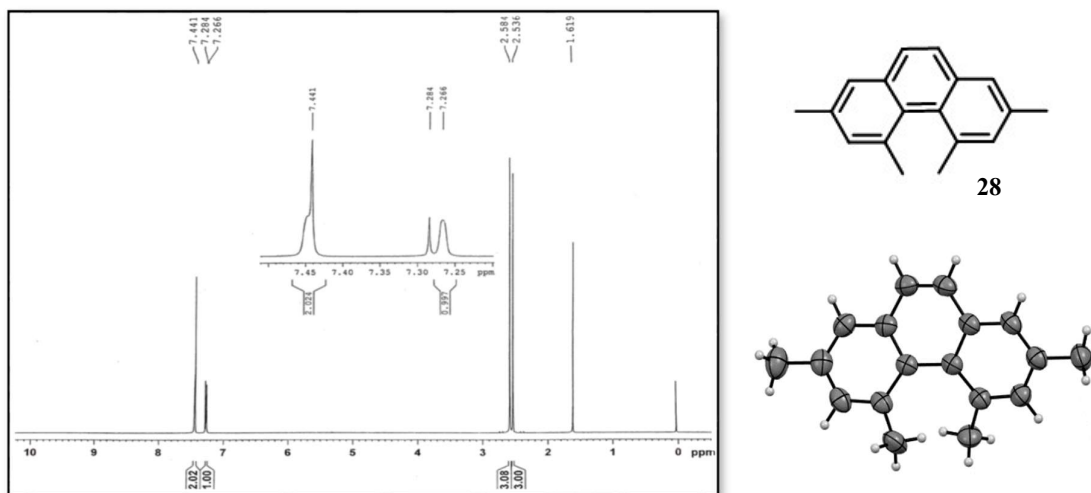
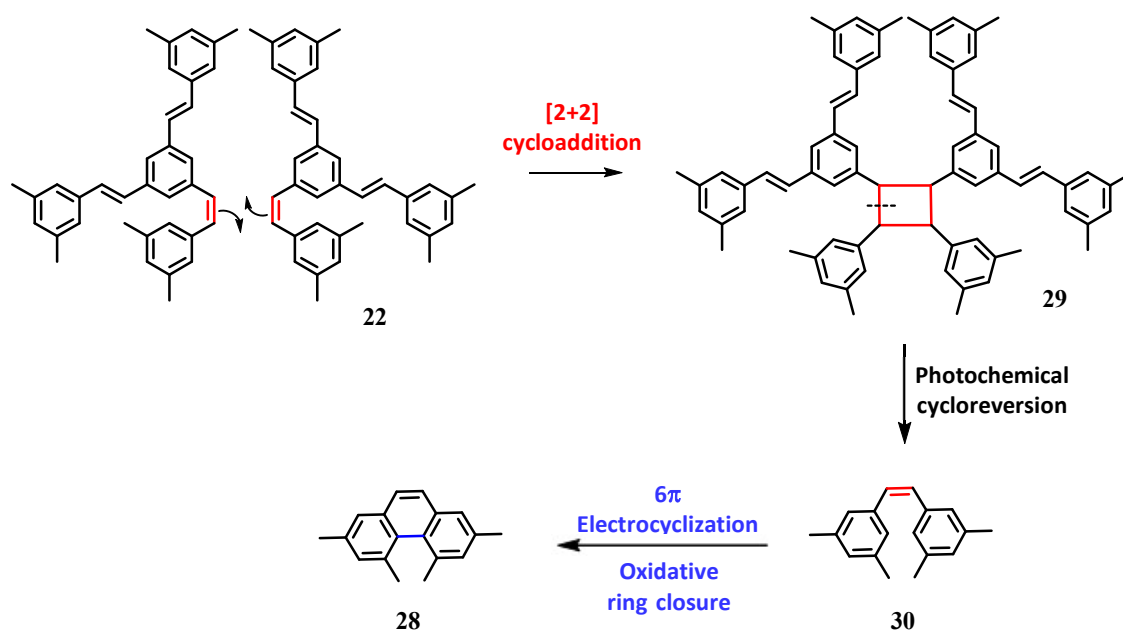


**Figure 4.9:**  $^1\text{H}$  NMR of **28** ( $\text{CDCl}_3$ ) (left) and ORTEP plot of compound **28** CCDC 152604 (right)

### 4.3.2.3 Possible mechanism for the formation of 28

It is well-known that photocyclization reactions should be carried out at concentrations of  $10^{-3}$  M and lower in order to avoid the competing photodimerization reactions.<sup>18</sup> This statement led us to propose this possible mechanism which could explain the formation of **28** in the best way (**Scheme 4.10**). An intermolecular [2+2] cycloaddition reaction between two molecules of **22** might have resulted into the formation of the cyclobutane derivative **29** which might have further undergone photochemical cycloreversion reaction to obtain olefin **30**. This cycloreversion presumably occurs through formation of radical intermediates, stabilized by the presence of aryl substituents. The olefin **30** thus formed subsequently undergoes electrocyclic ring closure to furnish the phenanthrene derivative **28**.



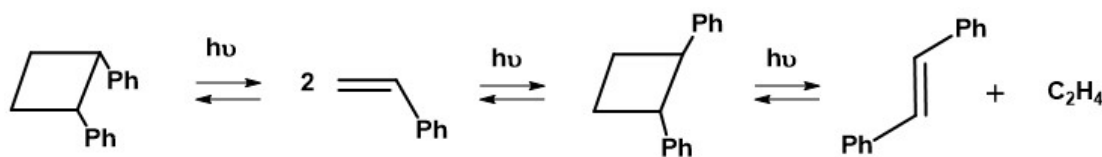
**Scheme 4.10:** Possible mechanism for the formation of 2,4,5,7-tetramethylphenanthrene

Such type of cyclobutane ring fission is not very common under photochemical conditions, although there are a few reports in the literature showing the possibility of this type of cleavage.

### 4.3.2.4 Photochemical cycloreversion: LITERATURE REPORTS

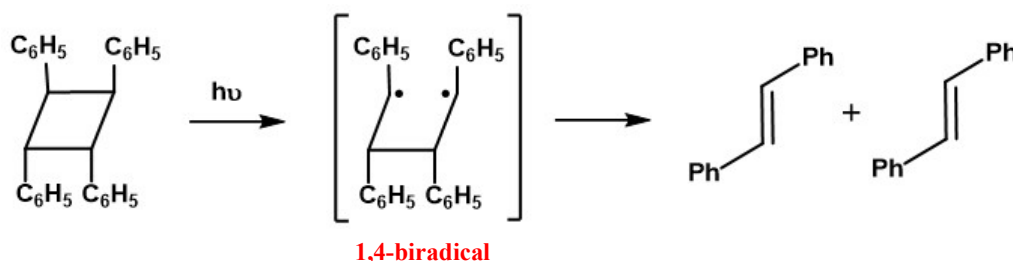
In 1974, while studying the orientation in the photochemical cleavages of cyclobutane ring, Kaupp has shown that there is a clear preference for the photochemical fission of the

cyclobutane bond bearing the substituent which causes steric hindrance (**Scheme 4.11**).<sup>19</sup>



**Scheme 4.11:** Photochemical cleavage of cyclobutane ring

Later in 1979, Shizuka and co-workers studied the photolysis of 1,2,3,4-tetraphenylcyclobutane in hydrocarbon solvents and observed that it proceeds via short-lived 1,4-biradicals (**Scheme 4.12**).<sup>20</sup>



**Scheme 4.12:** Photolysis of 1,2,3,4-tetraphenylcyclobutane

### 4.3.3 Attempt to synthesize propeller-shaped triple helical oxazine

In order to check whether such photochemical [2+2]cycloaddition and cycloreversion reactions occur in such [4]helicene systems, we designed a triple helical oxazine as our next target molecule as its retrosynthetic path involves one such photocyclization reaction. The synthesis of target molecule could be achieved by oxazine formation between a chiral amine and the configurationally unstable triple 2-hydroxy[4]helicene, which in turn can be obtained by demethylation of its corresponding methoxy derivative. The triple 2-methoxy[4]helicene could be obtained by photocyclization of the corresponding tris-olefin derivative (**Figure 4.10**).

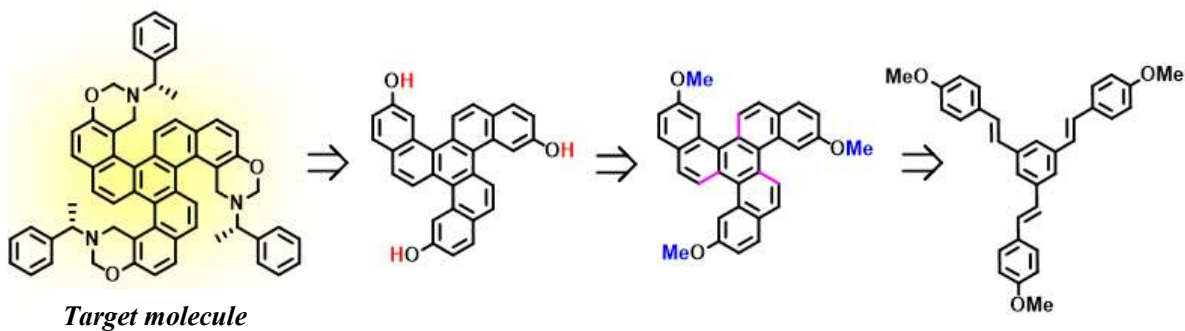
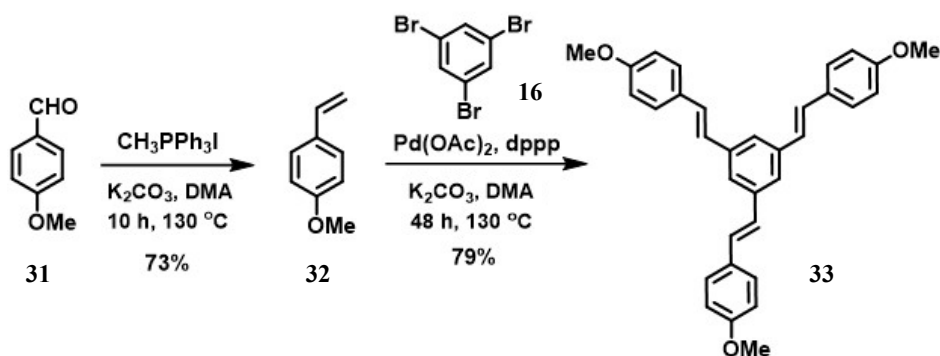


**Figure 4.10:** Retrosynthetic analysis of propeller-shaped helical oxazine



### 4.3.3.1 Synthesis of 1,3,5-tris((E)-4-methoxystyryl)benzene

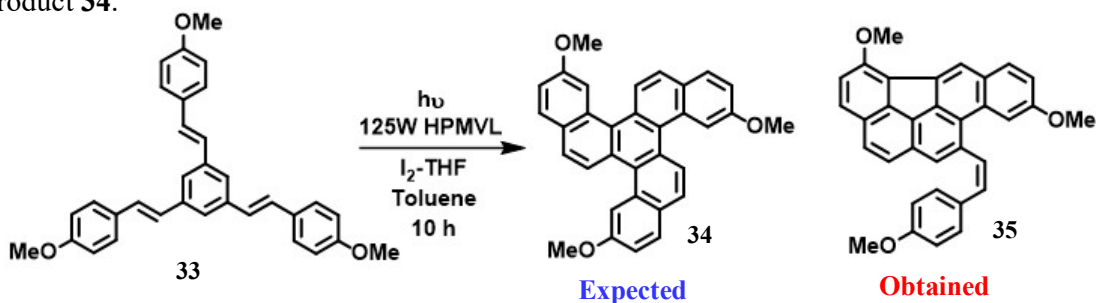
The tris-olefin **33** was synthesized by a stepwise Wittig-Heck approach. 4-methoxybenzaldehyde **31** was subjected to Wittig reaction with the one carbon Wittig salt to obtain *p*-methoxy styrene **32**. This styrene derivative **32** was purified by a filter column using silica gel column chromatography and further reacted with 1,3,5-tribromobenzene under Heck reaction conditions to obtain the desired tris-olefin **33** in good yield (**Scheme 4.13**).<sup>21</sup> The formation of **33** was confirmed by the <sup>1</sup>H NMR, which showed a 's' at 3.87 ppm indicating the presence of only one type of methoxy group as the compound **33** is symmetrical. Also, the presence of two 'd' at 7.17 and 7.04 (16.0 Hz) revealed the formation of *E*- isomer of **33**.



**Scheme 4.13:** Synthesis of tris-olefin **33**

### 4.3.3.2 Photocyclization of 1,3,5-tris((E)-4-methoxystyryl)benzene

The tris-olefin **33** was subjected to oxidative photocyclization under 125 W HPMVL, using iodine and tetrahydrofuran in toluene as solvent (**Scheme 4.14**). On completion of the reaction, the crude mass was purified by column chromatography using silica-gel, which gave a single pure product along with a mixture of some impurities. The isolated pure product was analyzed by different spectroscopic techniques. The <sup>1</sup>H NMR of which showed the presence of three different methoxy groups, thus indicating the lack of formation of our desired symmetrical product **34**.



**Scheme 4.14:** Photocyclization of tris-olefin **33**



The detailed analysis of this  $^1\text{H}$  NMR, indicated the formation of compound **35**. Moreover, the mass analysis and the HRMS were also in favor of formation of **35**. However, we were unsuccessful in obtaining a single crystal of compound **35**, structural parameters were obtained by Computational study. Also, it is difficult for us to predict the mechanism for the formation of this unexpected product **35**.

#### 4.3.3.3 Computational Analysis of compound 35

Computational analysis of compound **35** was carried out using the Gaussian 09 Software to obtain the electronic structures. The optimized geometry for **35** was computed using B3LYP function with 6-31G(d,p) basis set. The energies of the frontier molecular orbitals were calculated: -5.1335 eV for HOMO and -1.6193 eV for LUMO. According to which, the theoretical band gap was calculated to be 3.5 eV. The optimized geometry and the FMOs of **35** are as shown in **Figure 4.11**.

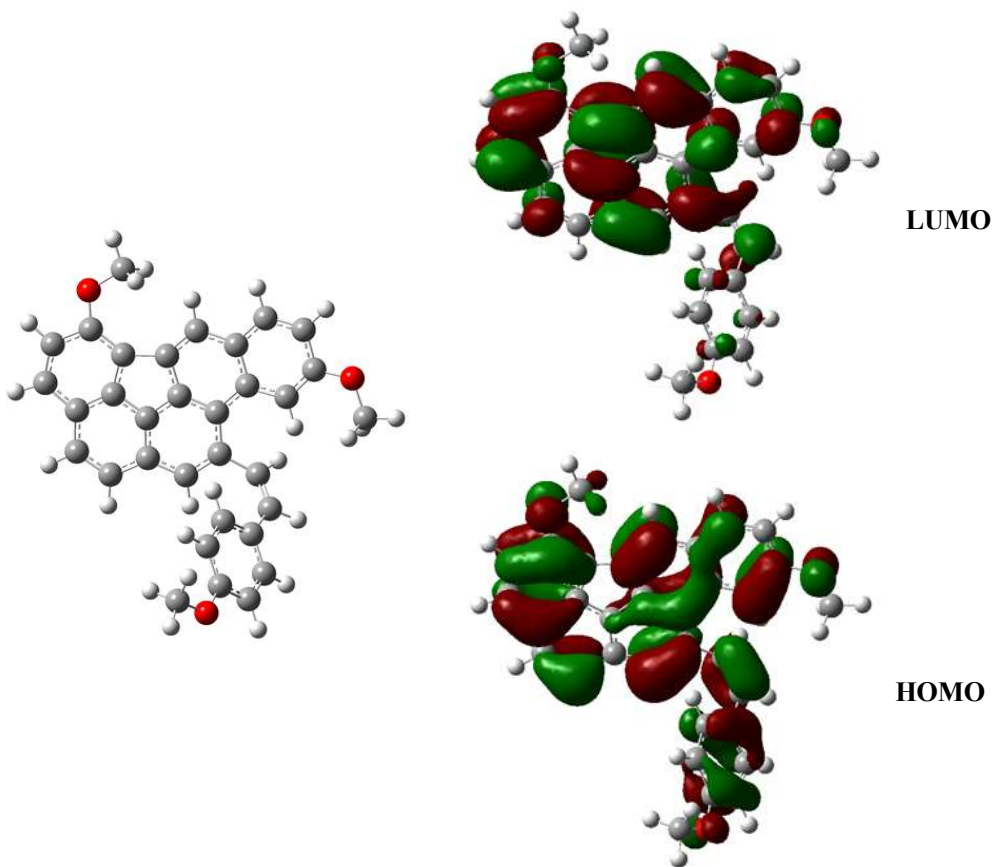


**Figure 4.11:** Optimized geometry and HOMO and LUMO orbitals of 35

## 4.4 Conclusion

The attempts for the synthesis of some propeller-shaped triple helicenes by oxidative photocyclization method are discussed in this chapter. Our first target was to synthesize triple aza[6]helicene, where the tris-olefin precursor was synthesized successfully, but further we failed to synthesize our target molecule. We thought that the steric strain caused by the bulky carbazole group might have hindered the usual cyclization process. So, the triple 1,3-dimethyl[4]helicene, which is comparatively a smaller moiety with lesser steric strain was chosen as our next target molecule. In the process of synthesizing this target molecule, we obtained an unexpected compound which was confirmed by single crystal X-ray analysis. The formation of this compound was explained by proposing a mechanism. Lastly, attempts to synthesize a triple helical oxazine are also discussed, where an unusually cyclized product was obtained.

## 4.5 Experimental Data

Reagents were purchased from Sigma-Aldrich Chemicals Limited, Sisco, Avara Chemicals Limited, etc., and were used without further purification. Thin layer chromatography was performed on Merck 60 F254 Aluminum coated plates. The spots were visualized under UV light or with iodine vapor. All the compounds were purified by column chromatography using SRL silica gel (60–120 mesh). All reactions were carried out under an inert atmosphere (nitrogen) unless other conditions are specified. NMR Spectra were recorded on a 400 MHz Bruker Advance 400 spectrometer (400 MHz for  $^1\text{H}$  NMR and 100 MHz for  $^{13}\text{C}$  NMR) with  $\text{CDCl}_3$  as the solvent and TMS as the internal standard. Signal multiplicity is denoted as singlet (s), broad singlet (bs), doublet (d), doublet of doublet (dd), triplet (t), doublet of triplet (dt), quartet (q), and multiplet (m). Mass spectra were recorded on a Thermo-Fischer DSQ II GCMS instrument. IR Spectra were recorded on a Perkin-Elmer FTIR RXI spectrometer as KBr pellets. Melting points were recorded in Thiele's tube using paraffin oil and are uncorrected.

### Synthetic procedures and analytical data

#### 2,4,6-Tribromoaniline (15)



**Molecular formula:**  $\text{C}_6\text{H}_4\text{Br}_3\text{N}$

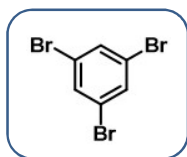
**Molecular weight:** 329.81

**Physical state:** brownish needles

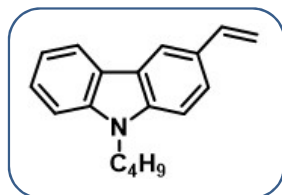
**M.p** = 120-122 °C

Dissolve 5 g (0.11 mol) of aniline in 15 mL of glacial acetic acid and stir well while running in slowly a solution of 26.4 g (17 mL, 0.33 mol) of bromine in 17 mL of glacial acetic acid. The beaker is to be cooled in ice during the addition as the reaction is exothermic. The final product is obtained by the addition of a little more bromine if necessary. Pour this mixture into excess of water, filtered and washed well with water, and dried. Recrystallize this crude mass with rectified spirit to obtain brownish needles of 2,4,6-tribromoaniline. The analytical data were in complete agreement with the previously published data.<sup>22</sup> **Yield:** 12.5 g (71%)

**$^1\text{H}$  NMR (400 MHz,  $\text{CDCl}_3$ ):**  $\delta$  4.57 (br s, 2H), 7.51 (s, 2H).

**1,3,5-Tribromobenzene (16)****Molecular formula:** C<sub>6</sub>H<sub>3</sub>Br<sub>3</sub>**Molecular weight:** 314.80**Physical state:** white crystalline solid**M.p.** = 122 °C

2,4,6-tribromoaniline (9.44 g, 0.03 mol) was dissolved in 60 ml of rectified spirit under constant heating in a two-necked flask fitted with a reflux condenser, the second neck being closed with a stopper. Add, from a burette or small graduated pipette, 5.3 g (3.5 mL) of concentrated sulphuric acid to the hot solution via the side-neck with constant stirring, replace the stopper and heat on a water bath until the clear solution boils. Remove the flask from the heating, and add 3.5 g (0.05 mol) of powdered sodium nitrite in two approximately equal portions via the side neck; after each addition, replace the stopper and shake the flask vigorously; when the reaction subsides, add the second portion of the sodium nitrite. Heat the flask on a boiling water bath as long as gas is evolved; shake well from time to time. Allow the solution to cool for 10 minutes, and then immerse the flask in an ice bath. A mixture of tribromobenzene and sodium sulphate crystallises out. Filter with suction on a Buchner funnel, wash with a small quantity of ethanol and then repeatedly with water to remove all the sodium sulphate. The crude obtained was purified on silica gel column using petroleum ether to afford **16** as white crystalline solid. The analytical data were in complete agreement with the previously published data.<sup>23</sup> **Yield:** 6.5 g (69 %)

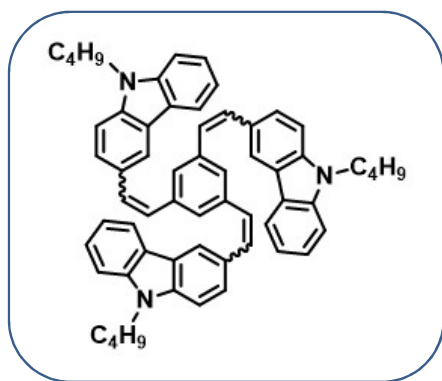
**3-Vinyl *N*-butyl carbazole (18)****Molecular formula:** C<sub>18</sub>H<sub>19</sub>N**Molecular weight:** 249.35**Physical state:** colourless viscous oil**B.p.** = above 250 °C

In a 100 mL flask equipped with a reflux condenser were placed 3-formyl *N*-butyl carbazole **17** (1.0 g, 3.98 mmol), methyl triphenylphosphonium iodide (2.41 g, 5.97 mmol), dry potassium carbonate (1.65 g, 11.95 mmol), and *N,N*-dimethylacetamide (20 mL). This mixture was heated under reflux for 48 h. After cooling, the mixture was poured to water and extracted with ethyl acetate (3×100 mL). The combined organic phase was washed with water and brine and dried over anhydrous sodium sulfate. The solvent was removed under reduced pressure, and the crude product was purified by column chromatography on silica gel using petroleum ether as eluent

to afford 3-vinyl *N*-butyl carbazole as colourless viscous oil. The analytical data were in complete agreement with the previously published data.<sup>24</sup> **Yield:** 0.76 g (77 %)

**<sup>1</sup>H NMR (400 MHz, CDCl<sub>3</sub>):** δ 0.89 (t, *J* = 4 Hz, 3H), 1.33 (m, 2H), 1.79 (m, 2H), 4.21 (t, *J* = 4 Hz, 2H), 5.17 (d, *J* = 8 Hz, 1H), 5.75 (d, *J* = 8 Hz, 1H), 6.89 (m, 1H), 7.19 (m, 1H), 7.29 (d, *J* = 4 Hz, 1H), 7.34 (d, *J* = 8 Hz, 1H), 7.42 (t, *J* = 8 Hz, 1H), 7.53 (d, *J* = 8 Hz, 1H), 8.07 (t, *J* = 8 Hz, 2H).

### 1,3,5-tris(2-(9-butyl-9*H*-carbazol-3-yl)vinyl)benzene (**19**)



**Molecular formula:** C<sub>60</sub>H<sub>57</sub>N<sub>3</sub>  
**Molecular weight:** 820.13  
**Physical state:** pale yellow solid  
**M.p** = 122 °C

A solution of palladium acetate (0.005 g, 0.026 mmol, 1.5 mol %) and 1,3-bis(diphenylphosphinopropane) (0.022 g, 0.053 mmol, 3 mol %) was prepared in *N,N*-dimethylacetamide (5 mL) under nitrogen atmosphere. The mixture was stirred at room temperature until a homogeneous solution was obtained. This catalyst solution was repeatedly purged by N<sub>2</sub> prior to use. A two-necked round bottom flask was charged with 1,3,5-tribromobenzene **16** (0.558 g, 1.77 mmol), dry potassium carbonate (1.22 g, 8.8 mmol) and *N,N*-dimethylacetamide (10 mL). The solution was repeatedly purged with N<sub>2</sub>. 3-vinyl *N*-butyl carbazole **18** (1.987 g, 7.97 mmol) was added at 60 °C and the mixture was heated up to 100 °C. At 100 °C, the previously prepared Pd catalyst solution was added drop wise and the mixture was further heated to 140 °C for 48 h. After the completion of the reaction, the mixture was poured into ice-cold water and extracted with dichloromethane (3 x 100 mL). The combined organic phase was washed with water, brine, and dried over anhydrous sodium sulfate. The solvent was removed under reduced pressure and the crude product was purified by column chromatography on silica gel using petroleum ether–ethyl acetate (98:2) as eluent to afford predominantly *E* isomer of **19** as light yellow solid. The analytical data were in complete agreement with the previously published data.<sup>25</sup> **Yield:** 0.841 g (58 %)

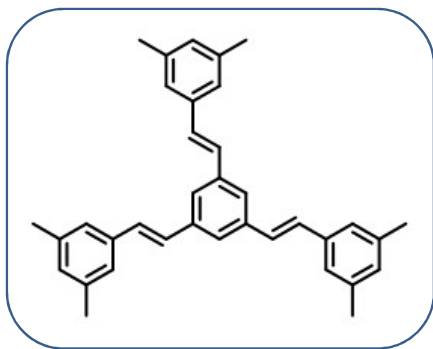
**<sup>1</sup>H NMR (400 MHz, CDCl<sub>3</sub>):** δ 8.28 (d, *J* = 1.2 Hz, 1H), 8.17 (d, *J* = 7.6 Hz, 1H), 7.71 (dd, *J*

= 8.4 and 1.2 Hz, 1H), 7.63–7.60 (m, 2H), 7.53–7.49 (m, 1H), 7.45–7.37 (m, 3H), 7.31–7.27 (m, 1H signal merged with water peak), 7.12 (d,  $J = 16.4$  Hz, 1H), 4.34 (t,  $J = 6.8$ , 2H), 1.93–1.86 (m, 2H), 1.48–1.39 (m, 2H), 0.98 (t,  $J = 7.2$  Hz, 3H).

### One Pot Oxidation-Wittig-Heck reaction to synthesize 22

A two-necked round bottom flask was charged with 1,3,5-tribromobenzene **16** (1.054 g, 3.34 mmol), 3,5-dimethylbenzyl bromide **21** (4.0 g, 20.09 mmol), methyl triphenyl phosphonium iodide (8.12 g, 20.09 mmol), potassium carbonate (6.94 g, 50.22 mmol), palladium acetate (0.022 g, 0.1 mmol, 3 mol%), triphenyl phosphine (0.052 g, 0.2 mmol, 6 mol%), and dimethyl sulfoxide (15 mL) under the nitrogen atmosphere. This mixture was slowly heated to 140 °C and continued for 24 h. The reaction mixture was quenched with water and extracted with ethyl acetate (3 X 25 mL). The combined organic phase was washed with water (2 X 20 mL), brine, and dried over anhydrous sodium sulfate. Solvent was removed in vacuum and the crude product was purified by column chromatography on silica gel to afford a mixture of stilbene derivatives.

#### **1,3,5-tris((*E*)-3,5-dimethylstyryl)benzene (22)**



**Molecular formula:** C<sub>36</sub>H<sub>36</sub>

**Molecular weight:** 468.68

**Physical state:** pale yellow solid

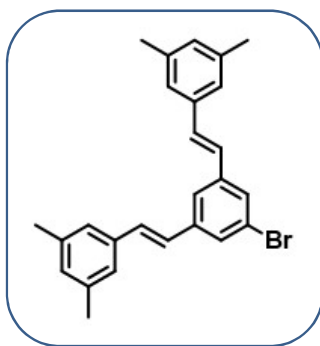
**M.p** = 240 °C

The analytical data were in complete agreement with the previously published data.<sup>26</sup> **Yield:** 0.35 g (24 %)

**<sup>1</sup>H NMR (400 MHz, CDCl<sub>3</sub>):** δ 7.56 (s, 1H), 7.22 (s, 2H), 7.17 (s, 2H), 6.97 (s, 1H), 2.39 (s, 6H).

**MS (DIP-El):**  $m/z$  468 (M<sup>+</sup>, 65%), 229 (41%), 151 (48%), 129 (54%), 119 (72%), 83 (77%), 55 (100%).

**5,5'-((1*E*,1'*E*)-(5-bromo-1,3-phenylene)bis(ethene-2,1-diyl))bis(1,3-dimethylbenzene) (23)**



**Molecular formula:** C<sub>26</sub>H<sub>25</sub>Br

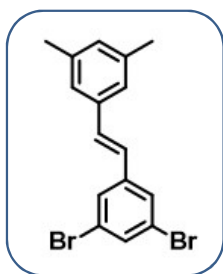
**Molecular weight:** 417.39

**Physical state:** white solid

**Yield:** 0.27 g (21 %)

**<sup>1</sup>H NMR (400 MHz, CDCl<sub>3</sub>):** δ 7.55 (d, *J* = 1.2 Hz, 2H), 7.52 (s, 1H), 7.18 (s, 4H), 7.11 (d, *J* = 16.0 Hz, 2H), 7.03 (d, *J* = 16.4 Hz, 2H), 6.98 (s, 2H), 2.38 (s, 12H).

**(*E*)-1,3-dibromo-5-(3,5-dimethylstyryl)benzene (24)**



**Molecular formula:** C<sub>16</sub>H<sub>14</sub>Br<sub>2</sub>

**Molecular weight:** 366.09

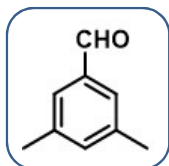
**Physical state:** white crystalline solid

**Yield:** 0.43 g (37 %)

**<sup>1</sup>H NMR (400 MHz, CDCl<sub>3</sub>):** δ 7.57 (d, *J* = 1.6 Hz, 2H), 7.54 (t, *J* = 1.6 Hz, 1H), 7.15 (s, 2H), 7.06 (d, *J* = 16.0 Hz, 1H), 6.98 (s, 1H), 6.92 (d, *J* = 16.4 Hz, 1H), 2.37 (s, 6H).

**Stepwise synthesis of 22**

**3,5-Dimethylbenzaldehyde (25)**



**Molecular formula:** C<sub>9</sub>H<sub>10</sub>O

**Molecular weight:** 134.17

**Physical state:** colourless oil

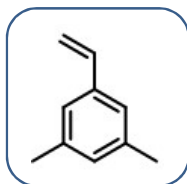
**B.p.** = 64-65 °C

In a 100 mL flask equipped with a reflux condenser were placed 3,5-dimethylbenzyl bromide **21** (2.0 g, 10.04 mmol), sodium bicarbonate (1.26 g, 15.07 mmol), and dimethyl sulfoxide (10 mL). This mixture was heated at 100 °C for 4 to 5 h. After cooling, the mixture was poured to excess of water and extracted with dichloromethane (3×50 mL). The combined organic phase

was washed with water and brine and dried over anhydrous sodium sulfate. The solvent was removed at low temperature, and the crude product was purified by a quick filter column on silica gel using petroleum ether/ ethyl acetate (95:05) as eluent to afford **25** as colourless oil. The analytical data were in complete agreement with the previously published data.<sup>27</sup> **Yield:** 1.29 g (96 %)

**<sup>1</sup>H NMR (400 MHz, CDCl<sub>3</sub>):**  $\delta$  2.37 (s, 6H), 7.24 (s, 1H), 7.47 (s, 2H), 9.93 (s, 1H).

### 3,5-Dimethylstyrene (**26**)



**Molecular formula:** C<sub>10</sub>H<sub>12</sub>

**Molecular weight:** 132.20

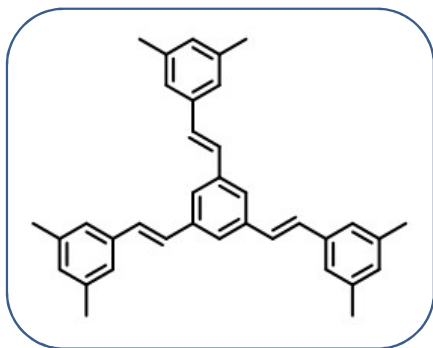
**Physical state:** colourless oil

**B.p.** = 57-58 °C

In a 100 mL flask equipped with a reflux condenser were placed 3,5-dimethylbenzaldehyde **25** (3.4 g, 25.33 mmol), methyl triphenylphosphonium iodide (12.29 g, 30.40 mmol), dry potassium carbonate (10.50 g, 76.01 mmol), and *N,N*-dimethylacetamide (20 mL). This mixture was heated to 130 °C for 8 h. After cooling, the mixture was poured to water and extracted with ethyl acetate (3×100 mL). The combined organic phase was washed with water and brine and dried over anhydrous sodium sulfate. The solvent was removed under reduced pressure, and the crude product was purified by column chromatography on silica gel using petroleum ether as eluent to afford 3-vinyl *N*-butyl carbazole as colourless viscous oil. The analytical data were in complete agreement with the previously published data.<sup>28</sup> **Yield:** 2.64 g (79 %)

**<sup>1</sup>H NMR (400 MHz, CDCl<sub>3</sub>):**  $\delta$  7.05-7.06 (m, 2H), 6.91-6.92 (m, 1H), 6.67 (dd, *J* = 17.6, 10.9 Hz, 1H), 5.74 (dd, *J* = 17.6, 1.0 Hz, 1H), 5.21 (dd, *J* = 10.9, 1.0 Hz, 1H), 2.33 (s, 6H).

### 1,3,5-tris((*E*)-3,5-dimethylstyryl)benzene (**22**)



**Molecular formula:** C<sub>36</sub>H<sub>36</sub>

**Molecular weight:** 468.68

**Physical state:** pale yellow solid

**M.p.** = 240 °C

A solution of 1,3,5-tribromobenzene **16** (0.250 g, 0.79 mmol), 3,5-dimethylstyrene **26** (0.62 g,

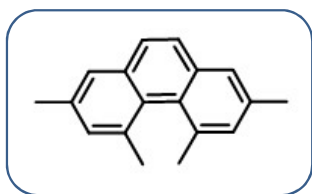


4.76 mmol), palladium acetate (0.005 g, 0.023 mmol, 3 mol%) and triphenylphosphine (0.022 g, 0.047 mmol, 6 mol%) was prepared in triethylamine (5 mL) in a sealed tube. The mixture was heated to reflux for 48 h. After the completion of the reaction, evaporate the trimethylamine and pour the mixture into ice-cold water and extracted with ethyl acetate (3 x 50 mL). The combined organic phase was washed with water, brine, and dried over anhydrous sodium sulfate. The solvent was removed under reduced pressure and the crude product was purified by column chromatography on silica gel using petroleum ether–ethyl acetate (98:2) as eluent to afford **22** as pale yellow solid. **Yield:** 0.24 g (65 %)

### Photocyclization of 22

In an immersion wall photoreactor equipped with a water cooling jacket and a stir bar, 1,3,5-tris((*E*)-3,5-dimethylstyryl)benzene **22** (0.340 g, 0.72 mmol), iodine (0.61 g, 2.39 mmol), and THF (7.85 g, 8.8 mL, 108.9 mmol) was dissolved in toluene (1200 mL). Nitrogen gas was bubbled through the solution within 10 min under sonication for removal of the dissolved oxygen prior to irradiation using a 125 W high-pressure mercury vapour (HPMV) lamp (12 h monitored by TLC). After completion of the reaction, the excess of iodine was removed by washing with aqueous Na<sub>2</sub>S<sub>2</sub>O<sub>3</sub> followed by distilled water. The organic layer was concentrated under the reduced pressure to obtain the crude product. The crude product purified by column chromatography over silica gel using petroleum ether as eluent to obtain a white solid.

### **2,4,5,7-Tetramethylphenanthrene (28)**



**Molecular formula:** C<sub>18</sub>H<sub>18</sub>

**Molecular weight:** 234.34

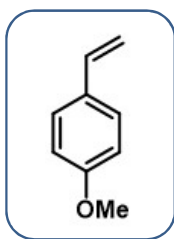
**Physical state:** white solid

**M.p** = 110-112 °C

The analytical data were in complete agreement with the previously published data.<sup>29</sup> **Yield:** 0.023 g (14 %)

**<sup>1</sup>H NMR (400 MHz, CDCl<sub>3</sub>):** δ 7.44 (bs, 1H merged with s, 1H), 7.27 (bs, 1H), 2.58 (s, 3H), 2.54 (s, 3H).

### ***p*-Methoxystrene (32)**



**Molecular formula:** C<sub>9</sub>H<sub>10</sub>O

**Molecular weight:** 134.18

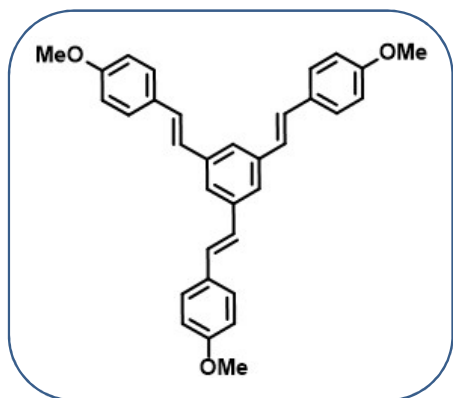
**Physical state:** colourless liquid

**B.p.** = 205 °C

In a 100 mL flask equipped with a reflux condenser were placed *p*-methoxybenzaldehyde **31** (2.0 g, 14.68 mmol), methyl triphenylphosphonium iodide (6.53 g, 16.15 mmol), dry potassium carbonate (6.09 g, 44.06 mmol), and *N,N*-dimethylacetamide (15 mL). This mixture was heated to 130 °C for 8 h. After cooling, the mixture was poured to water and extracted with dichloromethane (3×100 mL). The combined organic phase was washed with water and brine and dried over anhydrous sodium sulfate. The solvent was removed at low temperature, and the crude product was purified by column chromatography on silica gel using petroleum ether as eluent to afford *p*-methoxystyrene as colourless liquid. The analytical data were in complete agreement with the previously published data.<sup>30</sup> **Yield:** 1.44 g (73 %)

**<sup>1</sup>H NMR (400 MHz, CDCl<sub>3</sub>):** δ 7.33 (d, *J* = 8.5 Hz, 2H), 6.84 (d, *J* = 8.5 Hz, 2H), 6.65 (dd, *J* = 17.5, 10.5 Hz, 1H), 5.60 (d, *J* = 17.5 Hz, 1H), 5.11 (d, *J* = 11.0 Hz, 1H), 3.78 (s, 3H).

### 1,3,5-tris(*E*-4-methoxystyryl)benzene (**33**)



**Molecular formula:** C<sub>33</sub>H<sub>30</sub>O<sub>3</sub>

**Molecular weight:** 474.60

**Physical state:** white solid

A solution of 1,3,5-tribromobenzene **16** (0.796 g, 2.53 mmol), 4-methoxystyrene **32** (1.28 g, 9.53 mmol), palladium acetate (0.017 g, 0.076 mmol, 3 mol%) and triphenylphosphine (0.039 g, 0.15 mmol, 6 mol%) was prepared in triethylamine (2.5 mL) in a sealed tube. The mixture was heated to reflux for 48 h. After the completion of the reaction, evaporate the trimethylamine and pour the mixture into ice-cold water and extracted with ethyl acetate (3 x 50 mL). The combined organic phase was washed with water, brine, and dried over anhydrous sodium sulfate. The solvent was removed under reduced pressure and the crude product was purified

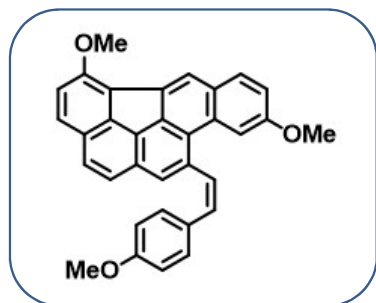
by column chromatography on silica gel using petroleum ether–ethyl acetate (90:10) as eluent to afford **33** as white solid. The analytical data were in complete agreement with the previously published data.<sup>21</sup> **Yield:** 0.94 g (79 %)

**<sup>1</sup>H NMR (400 MHz, CDCl<sub>3</sub>):** δ 7.53-7.51 (m, 3H), 7.17 (d, *J* = 16.4, 1H), 7.04 (d, *J* = 16.4 Hz, 1H), 6.95 (d, *J* = 8.8 Hz, 2H), 3.87 (s, 3H).

### Photocyclization of 33

In an immersion wall photoreactor equipped with a water cooling jacket and a stir bar, 1,3,5-tris((*E*)-4-methoxystyryl)benzene **33** (0.150 g, 0.31 mmol), iodine (0.26 g, 1.04 mmol), and THF (3.42 g, 3.85 mL, 47.46 mmol) was dissolved in toluene (650 mL). Nitrogen gas was bubbled through the solution within 10 min under sonication for removal of the dissolved oxygen prior to irradiation using a 125 W high-pressure mercury vapour (HPMV) lamp (10 h monitored by TLC). After completion of the reaction, the excess of iodine was removed by washing with aqueous Na<sub>2</sub>S<sub>2</sub>O<sub>3</sub> followed by distilled water. The organic layer was concentrated under the reduced pressure to obtain the crude product. The crude product purified by column chromatography over silica gel using petroleum ether as eluent to obtain an orange solid.

### **(*Z*)-5,9-dimethoxy-11-(4-methoxystyryl)indeno[4,3,2,1-*cdef*]chrysene (35)**



**Molecular formula:** C<sub>33</sub>H<sub>24</sub>O<sub>3</sub>

**Molecular weight:** 468.55

**Physical state:** orange solid

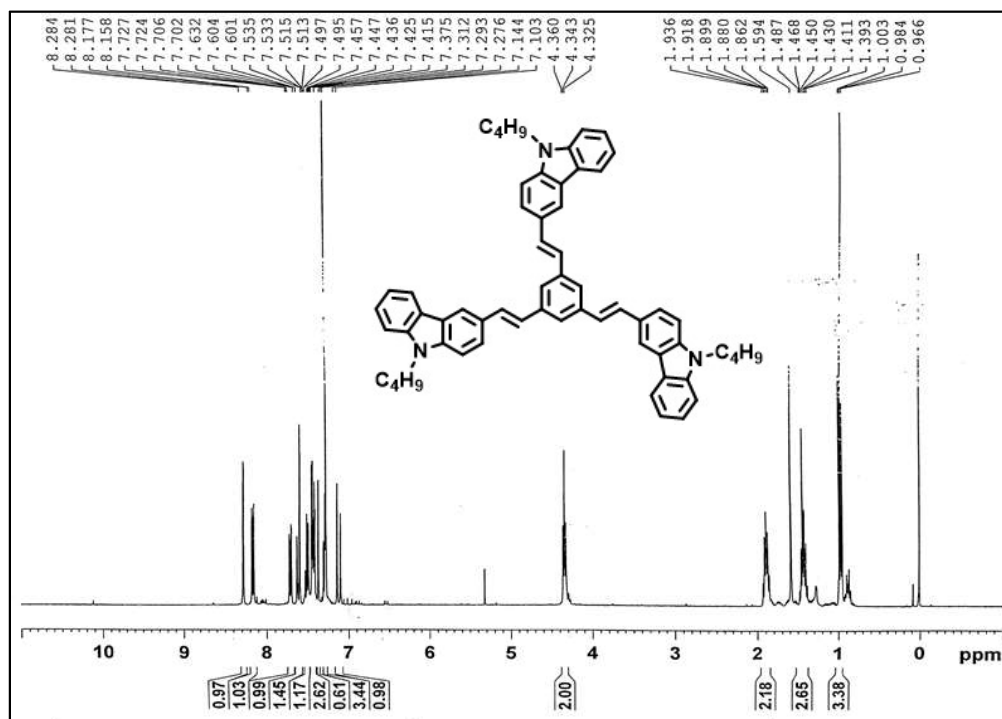
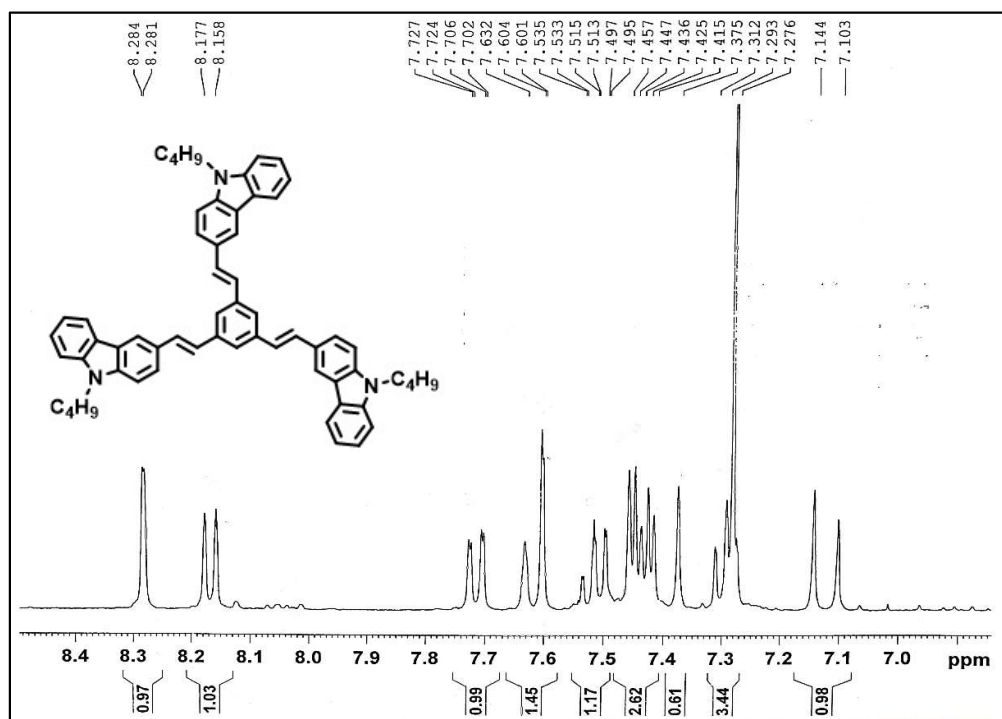
**<sup>1</sup>H NMR (400 MHz, CDCl<sub>3</sub>):** δ 9.35 (d, *J* = 9.6 Hz, 1H), 8.77 (d, *J* = 2.0 Hz, 1H), 8.51 (s, 1H), 8.42 (s, 1H), 8.26-8.23 (m, 2H), 7.99 (d, *J* = 8.8 Hz, 1H), 7.85 (d, *J* = 8.4 Hz, 1H), 7.82 (d, *J* = 8.8 Hz, 1H), 7.73-7.68 (m, 3H), 7.36 (dd, *J* = 8.8 and 2.8 Hz, 1H), 7.17 (d, *J* = 8.4 Hz, 2H), 4.22 (s, 3H), 4.10 (s, 3H), 3.99 (s, 3H).

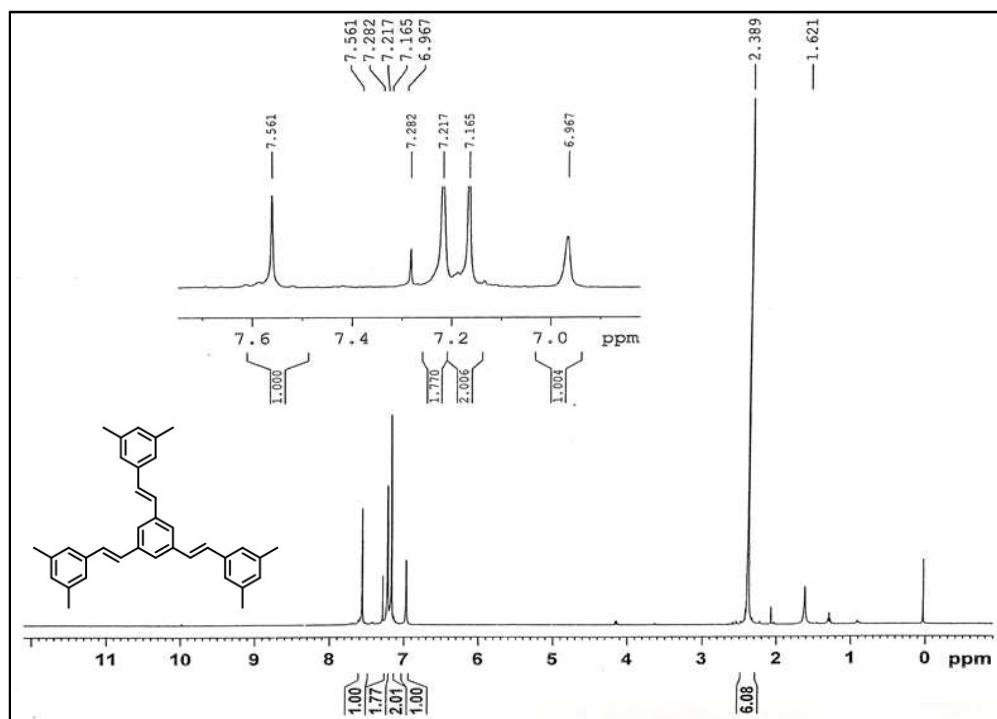
**IR (KBr):** 3035, 2930, 2827, 1610, 1511, 1494, 1459, 1428, 1356, 1250, 1220, 1194, 1092, 1026, 827, 790 cm<sup>-1</sup>.

**MS (DIP-El):** *m/z* 468 (M<sup>+</sup>, 7%), 257 (15%), 211 (21%), 183 (74%), 109 (26%), 98 (72%), 57 (100%).

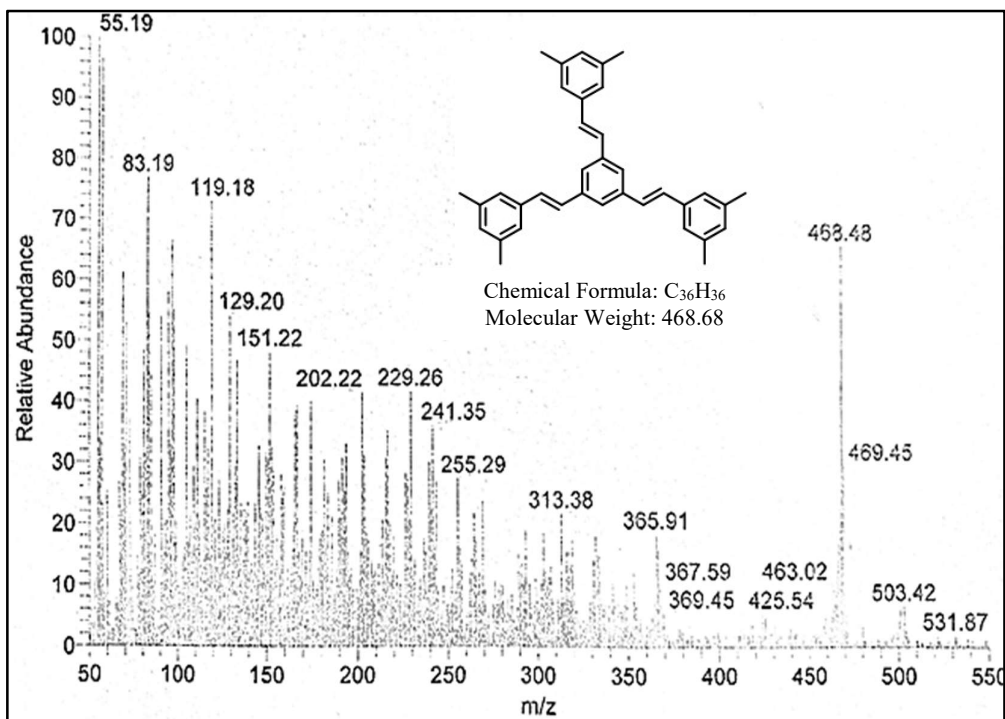
**HRMS (ESI<sup>+</sup>):** *m/z* calcd for C<sub>33</sub>H<sub>25</sub>O<sub>3</sub> [M+H]<sup>+</sup> 469.1721, found 469.1793.

## 4.6 Spectral Data

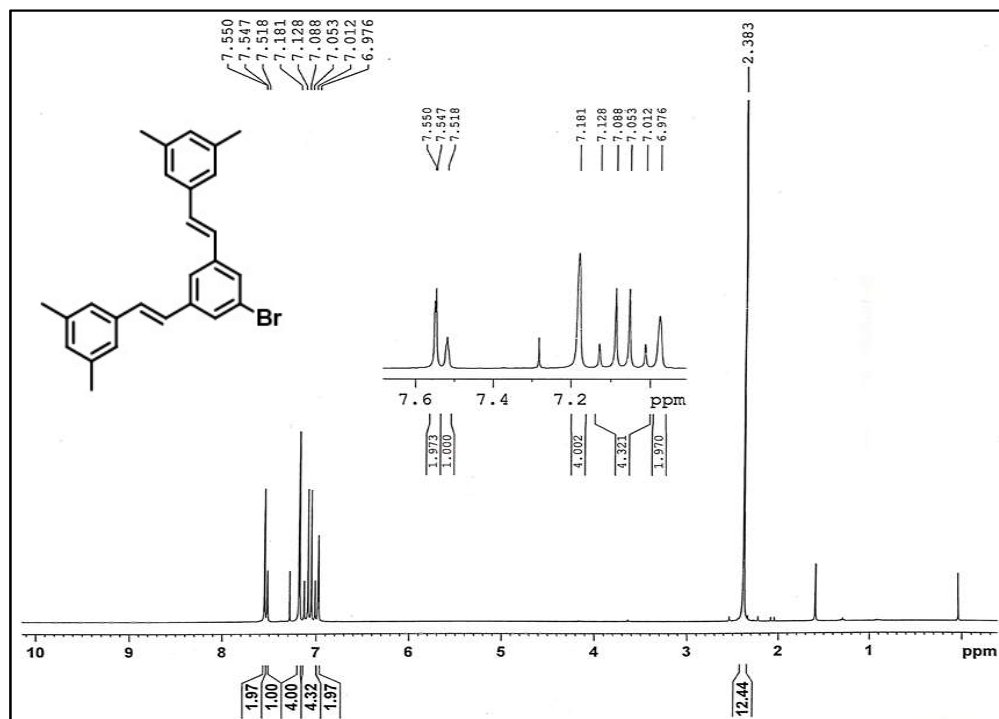
<sup>1</sup>H NMR Spectrum of 19 (CDCl<sub>3</sub>, 400 MHz)<sup>1</sup>H NMR Spectrum of 19 (CDCl<sub>3</sub>, 400 MHz) (enlarged aromatic region)



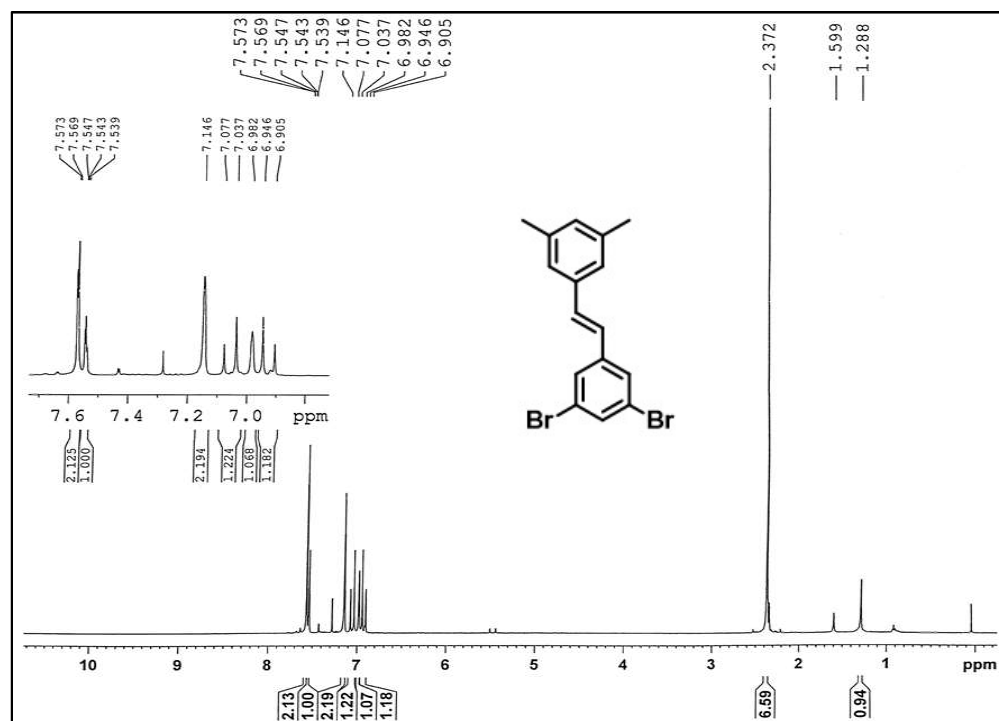
<sup>1</sup>H NMR Spectrum of 22 (CDCl<sub>3</sub>, 400 MHz)



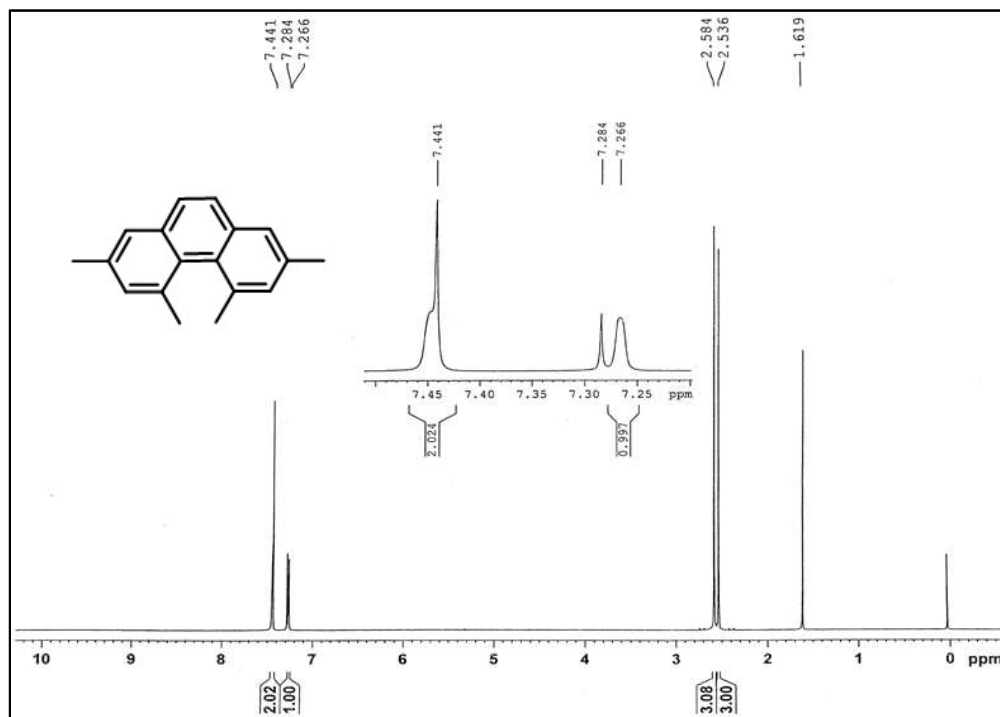
Mass Spectrum of 22



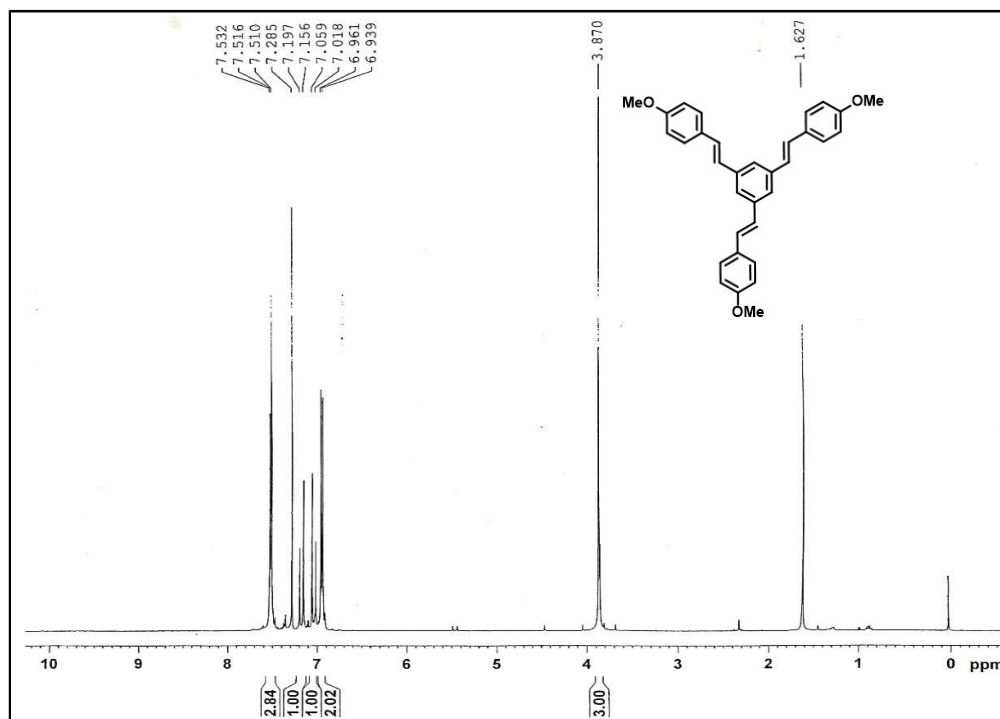
**<sup>1</sup>H NMR Spectrum of 23 (CDCl<sub>3</sub>, 400 MHz)**



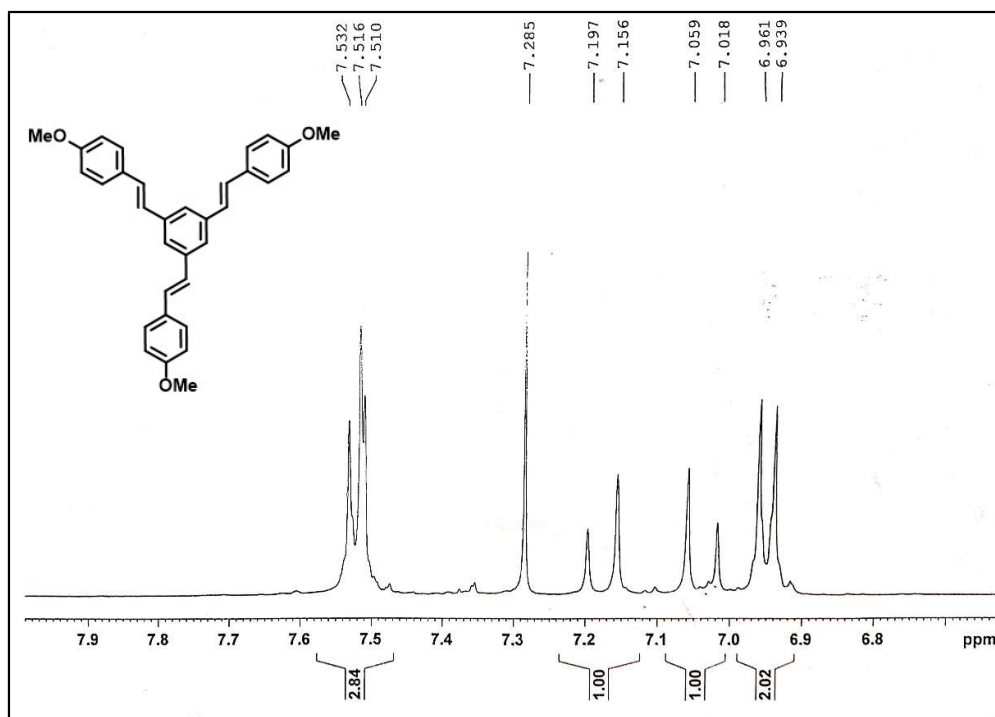
**<sup>1</sup>H NMR Spectrum of 24 (CDCl<sub>3</sub>, 400 MHz)**



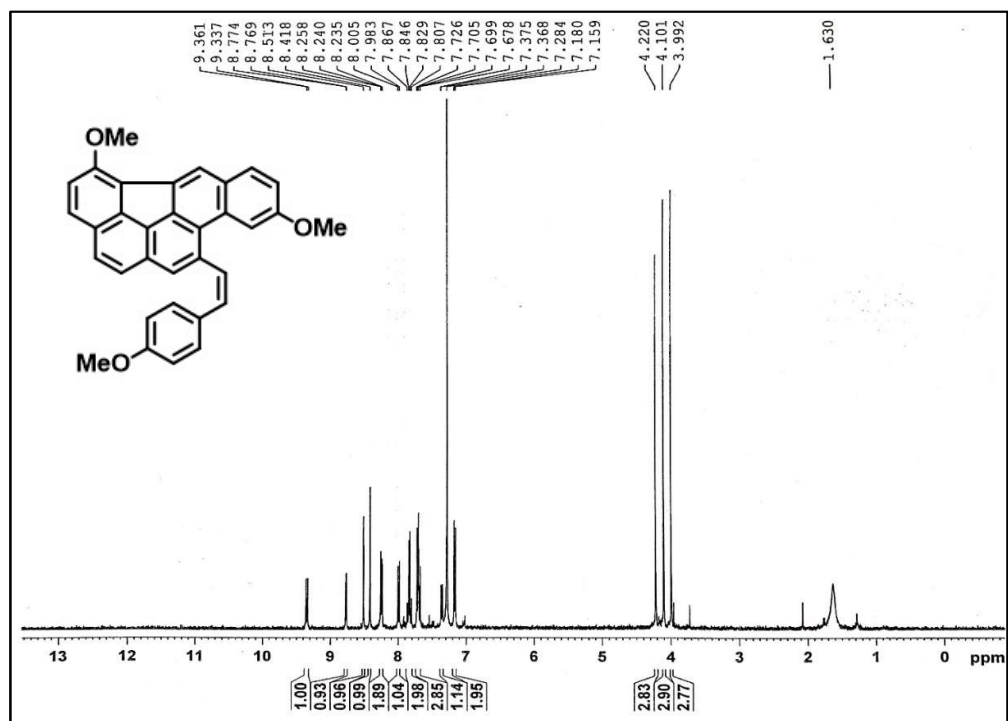
<sup>1</sup>H NMR Spectrum of 28 (CDCl<sub>3</sub>, 400 MHz)



<sup>1</sup>H NMR Spectrum of 33 (CDCl<sub>3</sub>, 400 MHz)

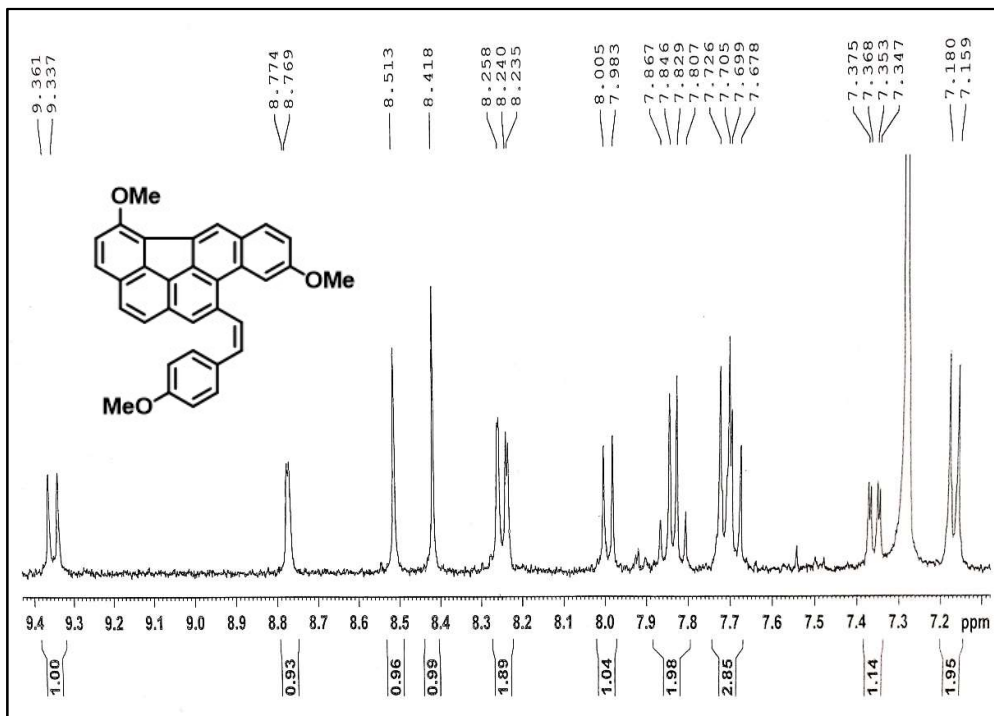


<sup>1</sup>H NMR Spectrum of 33 (CDCl<sub>3</sub>, 400 MHz) (Enlarged aromatic region)

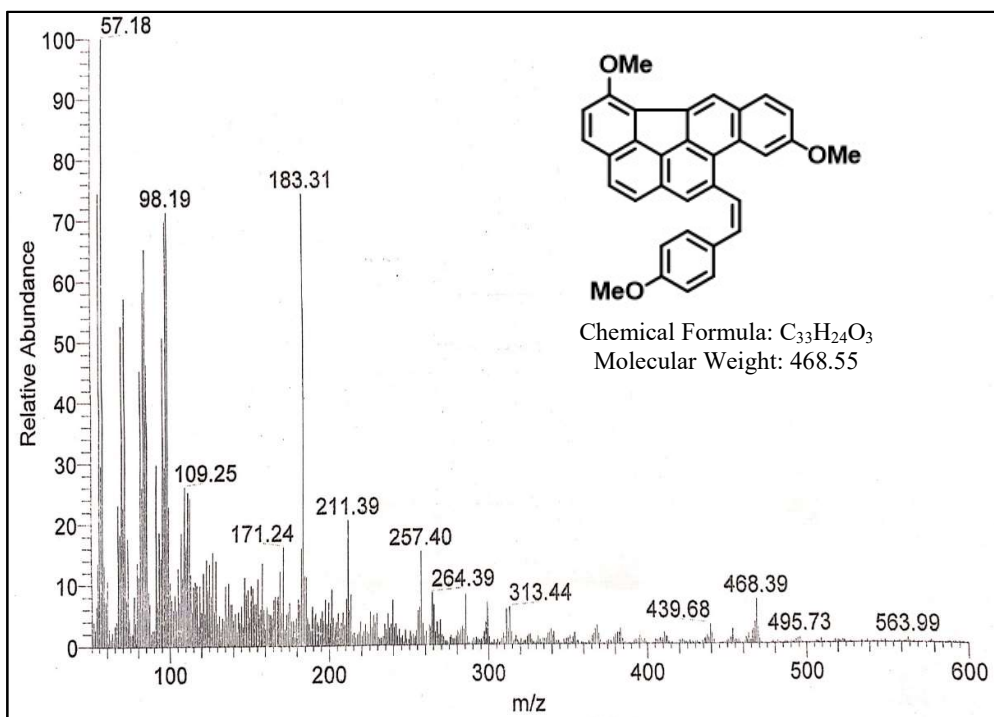


<sup>1</sup>H NMR Spectrum of 35 (CDCl<sub>3</sub>, 400 MHz)

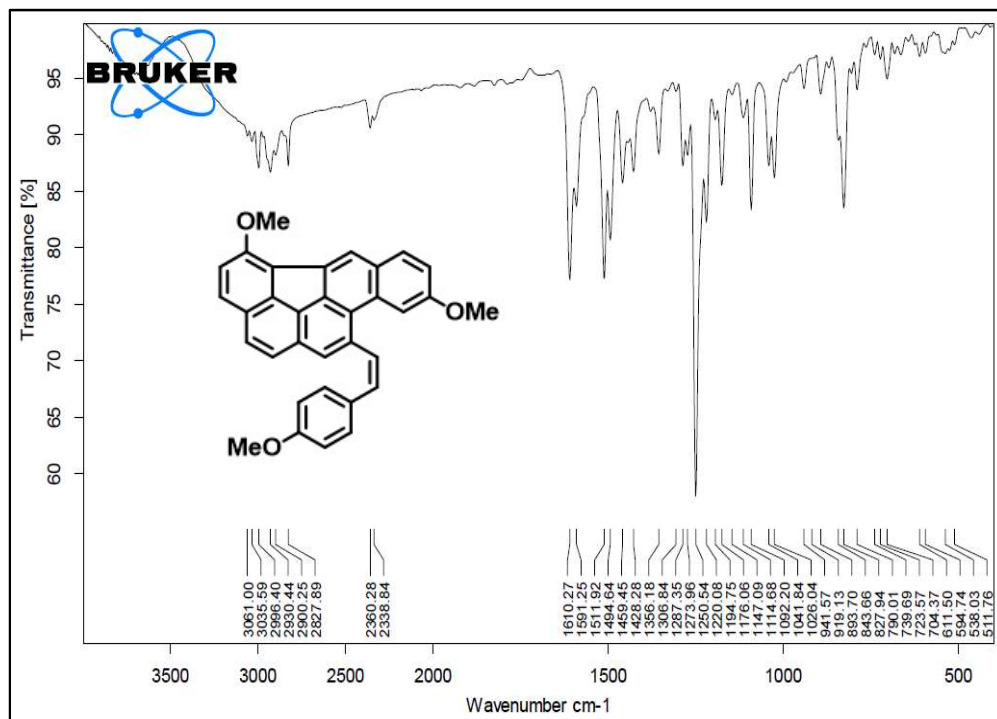




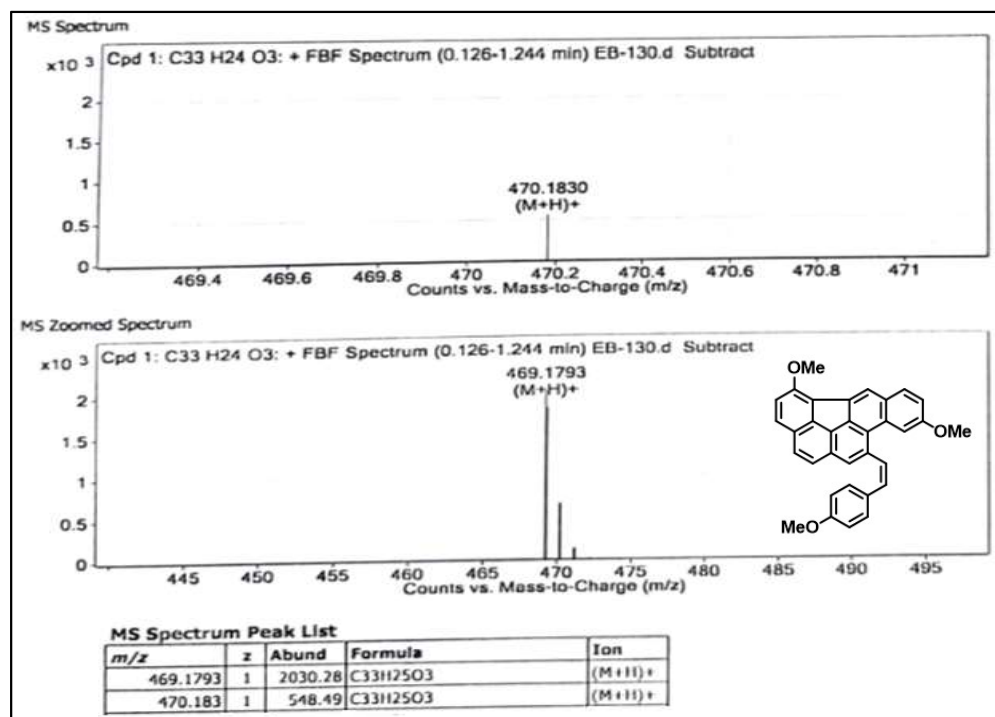
**<sup>1</sup>H NMR Spectrum of 35 (CDCl<sub>3</sub>, 400 MHz) (Enlarged aromatic region)**



**Mass Spectrum of 35**



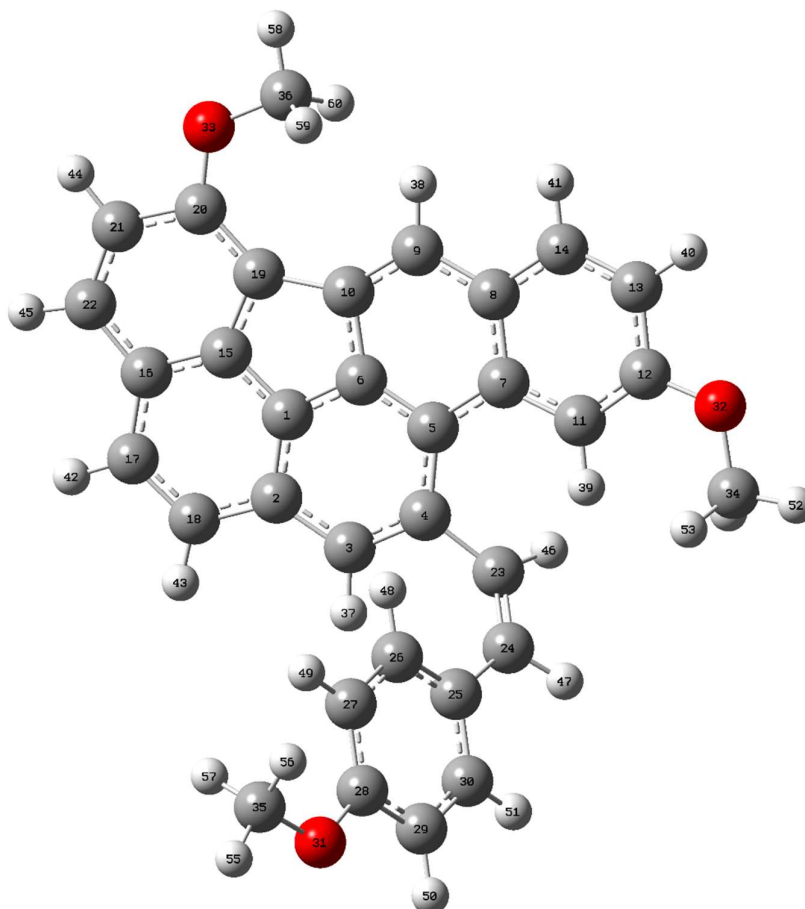
IR Spectrum of 35



HRMS Spectrum of 35

## 4.7 Computational Data

All DFT calculations were performed using Gaussian 09 Software.



Optimized geometry with numbering

### Cartesian co-ordinates of compound 50

Atom Numbers	Coordinates (Å)		
	X	Y	Z
1	-1.530963	-1.310264	-0.738597
2	-0.482585	-1.983394	-1.348008
3	0.642083	-1.156480	-1.644325
4	0.685859	0.204664	-1.324363
5	-0.430446	0.860184	-0.649914
6	-1.530494	0.041601	-0.397424

## Chapter-4

---

7	-0.566510	2.232603	-0.185637
8	-1.827230	2.612396	0.398155
9	-2.919517	1.693593	0.580619
10	-2.797892	0.379437	0.209482
11	0.466960	3.198139	-0.245163
12	0.268323	4.494022	0.209665
13	-0.979668	4.879058	0.746918
14	-1.989084	3.951237	0.838285
15	-2.756715	-1.881308	-0.372998
16	-2.994832	-3.235465	-0.613973
17	-1.924313	-3.967616	-1.244155
18	-0.724380	-3.380450	-1.599308
19	-3.610473	-0.898485	0.224115
20	-4.856928	-1.408925	0.610247
21	-5.146623	-2.796020	0.384178
22	-4.274033	-3.690535	-0.199462
23	1.852355	0.967799	-1.834542
24	3.169361	0.751107	-1.638312
25	3.871902	-0.175489	-0.737660
26	3.304342	-0.739408	0.416731
27	4.031077	-1.587588	1.250181
28	5.363311	-1.895868	0.944464
29	5.955553	-1.332061	-0.194352
30	5.220862	-0.483812	-1.008865
31	6.162088	-2.715597	1.686863
32	1.215330	5.474778	0.189803
33	-5.910363	-0.782073	1.200887
34	2.498974	5.159685	-0.329354
35	5.615039	-3.311395	2.853353
36	-5.846081	0.598029	1.515569
37	1.497702	-1.577530	-2.163737
38	-3.813452	2.102377	1.034425
39	1.431422	2.902354	-0.628733
40	-1.107436	5.900229	1.089511
41	-2.944074	4.241213	1.268947

---

## Chapter-4

---

42	-2.072505	-5.025106	-1.448898
43	0.044076	-3.983744	-2.074960
44	-6.129130	-3.123633	0.707765
45	-4.574148	-4.726095	-0.335036
46	1.595990	1.775460	-2.520780
47	3.841577	1.368452	-2.234513
48	2.279003	-0.506817	0.678634
49	3.553357	-1.994846	2.133243
50	6.990983	-1.570351	-0.413984
51	5.696678	-0.049596	-1.884665
52	3.087776	6.074610	-0.250906
53	2.984945	4.364110	0.248868
54	2.443815	4.853011	-1.381516
55	6.411700	-3.921490	3.281299
56	5.305511	-2.556360	3.587125
57	4.756907	-3.952893	2.616208
58	-6.804985	0.844905	1.974505
59	-5.042480	0.805960	2.229364
60	-5.713068	1.204984	0.614132

## 4.8 References

1. (a) Mori, T. Chiroptical Properties of Symmetric Double, Triple, and Multiple Helicenes, *Chem. Rev.* **2021**, *121*, 2373. (b) Hosokawa, T.; Takahashi, Y.; Matsushima, T.; Watanabe, S.; Kikkawa, S.; Azumaya, I.; Tsurusaki, A.; Kamikawa, K. Synthesis, Structures, and Properties of Hexapole Helicenes: Assembling Six [5]Helicene Substructures into Highly Twisted Aromatic Systems, *J. Am. Chem. Soc.* **2017**, *139*, 18512.
2. (a) Rickhaus, M.; Mayor, M.; Jurček, M. Strain-induced helical chirality in polyaromatic systems, *Chem. Soc. Rev.* **2016**, *45*, 1542. (b) Gingras, M. One hundred years of helicene chemistry. Part 1: non-stereoselective syntheses of carbohelicenes, *Chem. Soc. Rev.* **2013**, *42*, 968. (c) Shen, Y.; Chen, C.-F. Helicenes: Synthesis and Applications, *Chem. Rev.* **2011**, *111*, 1463.
3. (a) Naaman, R.; Paltiel, Y.; Waldeck, D. H. Chiral molecules and the electron spin, *Nat. Chem. Rev.* **2019**, *3*, 250. (b) Mondal, P. C.; Fontanesi, C.; Waldeck, D. H.; Naaman, R. Spin-Dependent Transport through Chiral Molecules Studied by Spin-Dependent Electrochemistry, *Acc. Chem. Res.* **2016**, *49*, 2560.
4. Jhulki, S.; Mishra, A. K.; Chow, T. J.; Moorthy, J. N. Helicenes as All-in-One Organic Materials for Application in OLEDs: Synthesis and Diverse Applications of Carbo- and Aza[5]helical Diamines, *Chem. Eur. J.* **2016**, *22*, 9375.
5. (a) Ravat, P.; Šolomek, T.; Jurček, M. Helicenes as Chiroptical Photoswitches, *ChemPhotoChem* **2019**, *3*, 180. (b) Ravat, P.; Šolomek, T.; Hussinger, D.; Blacque, O.; Jurček, M. Dimethylcethrene: A Chiroptical Diradicaloid Photoswitch, *J. Am. Chem. Soc.* **2018**, *140*, 10839. (c) Isla, H.; Crassous, J. Helicene-based chiroptical switches, *Comptes Rendus Chimie* **2016**, *19*, 39.
6. Hacker, N. P.; McOmie, J. F. W.; Meunier-Piret, J.; Van Meerssche, M. Benzocyclobutenes. Part 7. Synthesis and X-ray crystal structure of cyclobuta[I]phenanthrene-1,2-dione and the synthesis of hexabenz[a,c,g,i,m,o]triphenylene, *J. Chem. Soc., Perkin Trans. 1*, **1982**, 19.
7. Barnett, L.; Ho, D. M.; Baldrige, K. K.; Pascal, R. A. Jr. The Structure of Hexabenzotriphenylene and the Problem of Overcrowded “ $D_{3h}$ ” Polycyclic Aromatic Compounds, *J. Am. Chem. Soc.* **1999**, *121*, 727.
8. Peña, D.; Pérez, D.; Guitián, E.; Castedo, L. Synthesis of Hexabenzotriphenylene and

- Other Strained Polycyclic Aromatic Hydrocarbons by Palladium-Catalyzed Cyclotrimerization of Arynes, *Org. Lett.* **1999**, *1*, 1555.
9. Peña, D.; Cobas, A.; Pérez, D.; Guitián, E.; Castedo, L. Kinetic control in the palladium-catalyzed synthesis of C(2)-symmetric hexabenzotriphenylene. A conformational study, *Org. Lett.* **2000**, *2*, 1629.
  10. Bennett, A. A.; Kopp, M. R.; Wenger, E.; Willis, A. C. Generation of nickel(0) aryne and nickel(II) biphenyldiyl complexes via in situ dehydrohalogenation of arenes. Molecular structures of [Ni(2,2'-C<sub>6</sub>H<sub>4</sub>C<sub>6</sub>H<sub>4</sub>)(dcpe)] and C<sub>2</sub>-hexabenzotriphenylene, *J. Organomet. Chem.* **2003**, *667*, 8.
  11. Anirban, P.; Dechambenoit, P.; Bock, H.; Durola, F. Highly Twisted Arenes by Scholl Cyclizations with Unexpected Regioselectivity, *Angew. Chem. Int. Ed.* **2011**, *50*, 12582.
  12. Saito, H.; Uchida, A.; Watanabe, S. Synthesis of a Three-Bladed Propeller-Shaped Triple [5]Helicene, *J. Org. Chem.* **2017**, *82*, 5663.
  13. Fang, L.; Zhang, Y.; Ren, M.; Xie, X.; Li, T.; Yuan, Y.; Zhanga, J.; Wang, P. A triple helicene based molecular semiconductor characteristic of a fully fused conjugated backbone for perovskite solar cells, *Energy Environ. Sci.* **2022**, *15*, 1630.
  14. Zhou, F.; Huang, Z.; Huang, Z.; Cheng, R.; Yang, Y.; You, J. Triple Oxa[7]helicene with Circularly Polarized Luminescence: Enhancing the Dissymmetry Factors via Helicene Subunit Multiplication, *Org. Lett.* **2021**, *23*, 4559.
  15. Liu, J.; Jiang, L.; Chang, H.; Liu, H.; Cao, X.-Y.; Zou, Y.; Hu, Y. A C<sub>3</sub>-symmetric triple oxa[6]helicene with circularly polarized luminescence featuring parallel transition dipole moments, *Chem. Commun.* **2022**, *58*, 13087.
  16. (a) Newman, M. S.; Wise, R. M. The Synthesis and Resolution of 1,12-Dimethylbenzo[c]phenanthrene-5-acetic Acid, *J. Am. Chem. Soc.* **1956**, *78*, 450. (b) Lakshman, M. K.; Kole, P. L.; Chaturvedi, S.; Saugier, J. H.; Yeh, H. J. C.; Glusker, J. P.; Carrell, H. L.; Katz, A. K.; Afshar, C. E.; Dashwood, W.-M.; Kenniston, G.; Baird, W. M. Methyl Group-Induced Helicity in 1,4-Dimethylbenzo[c]phenanthrene and Its Metabolites: Synthesis, Physical, and Biological Properties, *J. Am. Chem. Soc.* **2000**, *122*, 12629.
  17. Saiyed, A. K.; Patel, K. N.; Kamath, B. V.; Bedekar, A. V. Synthesis of stilbene analogues by one-pot oxidation-Wittig and oxidation-Wittig–Heck reaction, *Tetrahedron Letters* **2012**, *53*, 4692.

18. Zertani, R.; Meier, H. Photochemistry of 1,3-distyrylbenzene. A new route to syn-[2.2](1,3)cyclophanes, *Chem. Ber.* **1986**, *119*, 1704.
19. Kaupp, G. Orientation in Photochemical Cyclobutane Cleavages : *cis*-Effect, *Angew. Chem. Int. Ed.* **1974**, *13*, 817.
20. Shizuka, H.; Seki, I.; Morita, T.; Iizuka, T. Photolyses of Tetraphenylcyclobutanes at 254 nm, *Bull. Chem. Soc. Jpn.* **1979**, *52*, 2074.
21. Amoroso, A. J.; John P. Maher, J. P.; McCleverty, J. A.; Ward, M. D. Magnetic spin exchange interactions between several metal centres in paramagnetic complexes with new polynucleating bridging ligands, *J. Chem. Soc.* **1994**, 1273.
22. Choi, H. Y.; Chi, D. Y. A Facile Debromination Reaction: Can Bromide Now Be Used as a Protective Group in Aromatic Systems?, *J. Am. Chem. Soc.* **2001**, *123*, 9202.
23. Vetter, W.; Armbruster, W.; Betson, T. R.; Schleucher, J.; Kapp, T.; Lehnert, K. Baseline isotopic data of polyhalogenated compounds, *Anal. Chim. Acta* **2006**, *577*, 250.
24. Aich, K.; Das, S.; Goswami, S.; Quah, C. K.; Sarkar, D.; Mondal, T. K.; Fun, H. –K. Carbazole–benzimidazole based dyes for acid responsive ratiometric emissive switches, *New J. Chem.* **2016**, *40*, 6907.
25. Cho, M. J.; Lee, T. W.; Kim, H. S.; Jin, J.- I.; Choi, D. H.; Kim, Y. M.; Ju, B.-, K. Syntheses and photophysical properties of new carbazole-based conjugated multi-branched molecules, *Macromol. Res.* **2005**, *15*, 595.
26. Nierle, J.; Kuck, D. Synthesis of a Benzoannelated Spheriphane (Globular Cyclophane) on the Way to Potential Precursors of C<sub>60</sub>-Fullerene, *Synlett.* **2006**, *18*, 2914.
27. Prebil, R.; Stavber, G.; Stavber, S. Aerobic Oxidation of Alcohols by Using a Completely Metal-Free Catalytic System, *Eur. J. Org. Chem.* **2014**, *2014*, 395.
28. Haubenreisser, S.; Wöste, T. H.; Martínez, C.; Ishihara, K.; Muñiz, K. Structurally Defined Molecular Hypervalent Iodine Catalysts for Intermolecular Enantioselective Reactions, *Angew. Chem. Int. Ed.* **2016**, *55*, 413.
29. Newman, M. S.; Lilje, K. C. Synthesis of 9-bromo derivatives of 4,5-, 2,7-, and 3,6-dimethyl- and 2,4,5,7- and 3,4,5,6-tetramethylphenanthrenes, *J. Org. Chem.* **1979**, *44*, 4944.
30. Hussain, M. I.; Feng, Y.; Hu, L.; Deng, Q.; Zhang, X.; Xiong, Y. Copper-Catalyzed Oxidative Difunctionalization of Terminal Unactivated Alkenes, *J. Org. Chem.* **2018**, *83*, 7852.